A common European approach to the regulatory testing of nanomaterials

NANoREG

Grant Agreement Number 310584

Deliverable D 3.02

Dustiness of carbon nanotubes using three different methods

Due date of deliverable: *2016/08/31*

Actual submission date: *2016/12/10*

Author(s) and company:	Olivier Witschger (INRS), Claire Dazon (INRS), Raphael Payet (INRS), Sébastien Bau(INRS), Ismo Kopponen (NRCWE), Dirk Brossel (BAuA), Keld Jensen (NRCWE)
Work package/task:	WP3 / Task3 3.2
Document status:	draft / final
Confidentiality:	confidential / restricted / public
Key words:	Dustiness, aerosol, characterization,

DOCUMENT HISTORY

Version	*Date*	*Reason of change*
1	2016/09/27	1st draft
2	2016/12/10	Final version
3	2017/03/08	Project Office harmonized lay-out
4	2017/06/13	Project Office adjusted figures to avoid blackening in PDF/A format

This project has received funding from the European Union Seventh Framework Programme (FP7/2007-2013) under grant agreement no 310584

Lead beneficiary for this deliverable: Institut National de Recherche et de Sécurité, INRS, partner 21

Owner(s) of this document	
Owner of the content	INRS, Partner 21
Co-Owner 1	NRCWE, Partner 4
Co-Owner 2	BAuA, Partner 3

Table of Content

1 Description of task

This task is involved in the characterization of nanomaterials as well as in the evaluation of exposures in the workplaces, particularly those resulting from the handling of nanomaterials in powder form. Thus, it aims to provide some answers to the proposed refined set of key questions from a regulatory perspective to be addressed in NANoREG. In particular questions:

- 2 on the measurement and characterization,
- 11 and 12 on exposure,
- 15 on risk management.

In that context, this task was to:

- In one part, develop further the Vortex Shaker (VS) and Small Rotating Drum (SRD) dustiness methods, two methods that have been the focus of attention for few years in various EU projects, including an on-going standardization CEN project.
- On the other part, to develop a new method, referred to as the Vibrofluidization (VF) method.

In performing this task, experimental tests were carried out with the three methods on a variety of carbon nanotubes (CNT) provided through the NanoREG project by JRC

2 Description of work & main achievements

2.1 Summary

Dustiness is a generic term addressing the ability of a powered material (e.g., loose, granulated, or pelletized powder) to generate an aerosol (airborne particles) during its handling. The dustiness of a powder is an important determinant for worker exposure and should be considered during the design and operation of many industrial or research processes [1]. For some years now, the dustiness is a requested input parameter in control banding (CB) tools to evaluate and control the risk of exposure to nanomaterials [2, 3]. It also starts to be of use in risk assessments, as for example recently on the carbon nanotube group [4].

In response to the special requirements associated with testing and measuring dustiness of nanomaterials, a number of recent studies have already aimed either at modifying the two methods (i.e. rotating drum and continuous drop) described in the EN15051-1 European standard [5] or at developing new approaches [6]. Among these, there is the Vortex Shaker (VS) and the Small Rotating Drum (SRD) methods developed in this work. The motivations that led to establish new method essentially relies on: simulating different (including worst-case) scenarios in a workplace from those claimed by the EN15051-1 methods [5]; performing dustiness experiments with a small amount of nanomaterial that are either potentially very toxic and/or costly; developing smaller setups that can be used in ventilated enclosures or fume hoods, thus better protecting operators in charge of experiments; to provide new relevant dustiness indices as well as information on size distribution and morphology, which are important elements to consider in risk assessments.

In that context, the objectives to this work were:

- To develop further the Vortex Shaker (VS) and Small Rotating Drum (SRD) dustiness methods, two methods that have been the focus of attention for few years in various EU projects, including an on-going standardization CEN project.
- To develop a new method, referred to as the Vibrofluidization (VF) method.

These developments were to apply within the framework of the NanoREG project to the case of carbon nanotubes. The main reason was that handling of CNT is a plausible scenario over their entire life-cycle, but for which exposure data obtained at workplaces are unfortunately scarce. Thus, it was hoped that the dustiness data produced could feed the future risk assessments by providing input parameters to exposure modeling or control banding tools.

The VS consists of a stainless steel tube (volume ≈ 100 cm^3) that is continuously shaken in a circular orbital motion, and in which a small volume (0.5 cm^3) of the powder sample is placed for testing. The SRD method involves the continuous multiple lifting and dropping of the powder sample (2 – 6 g) in a slow horizontal winnowing current of air (≈ 0.9 cm/s). The VF method is based on the use of specially designed vibrating fluidized bed where the mechanical vibration is characterized by a vertical shaking displacement whose amplitude and frequency are controlled. In the VF method, the test sample is positioned on a sintered metal frit held in a metal cylinder which is traversed by a low flowrate of HEPA-filtered air speed from 0.03 to about 0.1 cm/s at the level of the bed. For each method, the measurement part includes real-time instruments and sampling devices for electron microscopy (EM) analysis and / or gravimetric analysis. Specific protocols have been developed by each partner regarding sample preparation, sequence of the tests, and evaluation of the data.

The core multi-walled carbon nanotubes (MWCNT) NM400 and NM 401 have been tested by the three partners. The core single-walled carbon nanotube (SWCNT) NM 46000a has been tested by INRS and NRCWE. Among the alternatives MWCNT, 10 have been tested by INRS.

New standard parameters are proposed in this work to qualify the dustiness of powders, including the number- and mass-based dustiness indices, airborne particle emission rate as well as number-weighted size distribution of the emitted aerosol.

Overall, results show good reproducibility for each method. However, significant variations in dustiness indices and size distributions are observed between in the different methods.
The number-based and mass-based dustiness indices of the investigated CNTs present a large span over several orders of magnitude. It can be noted from the data obtained from the VS that ranking is different if the reference is the number or mass parameter. Released aerosols are polydisperse with number-weighted size distributions covering the range from about 50 nm to about 10 µm in aerodynamic equivalent diameter. These results are confirmed qualitatively by electron microscopy observations.

It is clear from this project that further work should be carried out to improve harmonization of dustiness methods, and implement them with other type of nanomaterials. Such work should allow in the future to perform pertinent inter-comparisons between methods and to develop a generic ranking approach to be used in occupational exposure assessment tools.

However, the experience gained in this project with VS and SRD methods directly contributes to the ongoing development of CEN / TC 137 standards in this area. Indeed, first working drafts on the VS and SRD have been prepared by Technical Committee CEN/TC 137 “Assessment of workplace exposure to chemical and biological agents”, and the CEN enquiry should start mid-2017.

Moreover, by proposing new relevant dustiness indices in different metrics (number and mass) as well as information on size distribution and morphology, the methods developed provide information about determinant of occupational exposure (element for NanoREG question 11) as well as input parameters for exposure modeling (element for NanoREG question 12). This contributes also to the need for improvement or development of control banding tools to incorporate these new input parameters (element for NanoREG question 15).

Finally, as element of response to NanoREG question 2, the obtained data reveal that:

- A ranking does exist between the tested CNT; the ranking is different whether the two dustiness metrics (number or mass) are considered, with no correlation between them.
- Released airborne CNTs are mostly released as bundles of different shapes and sizes that spread over the range from few tens of nanometers up to tens of micrometers.

2.2 Background of the task

Dustiness is a term addressing the ability of a powdered material (e.g., loose, granulated, or pelletized powder) to generate an aerosol (airborne particles) during agitation [5]. The dustiness of a powder is an important determinant for worker exposure and should be considered during the design and operation of many industrial or research processes [1]. The dustiness is then directly linked to several of the regulatory questions, as indicated in chapter 2.1.

Dustiness methods have been recommended for nanomaterials exposure assessment by the Organization for Economic Co-operation and Development [7]; they are also considered as important methods by the RIP-oN 2 project on the key aspects of the implementation of REACH with regard to nanomaterials [8]; moreover dustiness information is already in use as an input parameter in some control banding tools for nanomaterials and exposure models [2-4, 9, 10]. Finally, dustiness data can be seen as part of a safer by design approach as they provide the manufacturers of nanomaterials with information that can help improve their products (e.g. by selecting less dusty nanomaterials) or the users to improve their processes or their technical risk management approaches [11-13].

Dustiness is not an intrinsic physically or chemically defined property of a powder; its level depends on the physicochemical properties of the powder as well as the particles that compose the powder, the environmental conditions during testing and the energy supplied in the test bench that simulates a given handling or release scenario. As dustiness levels are expected to vary considerably with the test method, dustiness testing must be performed using well-defined methods and procedures to ensure reliable comparisons or ranking of materials [6].

In the context of occupational health risk assessment, as described in the in the part 1 of the EN 15051 standard [5], dustiness is defined as the ratio of the amount (mass within a given health-related fraction) of dust emitted during the test procedure to the amount of material used (i.e. mg/kg), and is classified according to three categories based on the mass fractions in each health-related fraction (inhalable, thoracic, respirable). In the EN15051 standard, two methods are proposed:

- The rotating drum (RD) method which involves the continuous multiple lifting and dropping of a sample of the bulk material in a slow horizontal winnowing current of air (≈ 0.9 cm/s). The dust released from dropping bulk material is conducted by the airflow (38 l/min) to a sampling section where it is separated aerodynamically into the three health-related

fractions by horizontal elutriation and inertial impaction in two stages made of porous metal foam. A fixed volume (35 cm^3) of sample material is required per test. The method and SOP are described in the part 2 of the EN15051 standard [14].

- The continuous drop (CD) method which involves the continuous dropping of bulk material in a slow vertical air current (5 cm/s). The dust released from dropping bulk material is conducted by the airflow to a sampling section where it is separated aerodynamically into the inhalable and respirable fractions. Between 60 g to about 100 g of sample material is required per test. The method and SOP are described in the part 3 of the EN15051 standard [15].

The EN15051 standard requires that:

- The sample materials are to be tested in the state 'as they are used', which means without any pre-conditioning step. However, the moisture content and the bulk density are determined prior to the tests.
- At least five replicate tests are required and the following test conditions shall apply: relative humidity (RH): (50 ± 10) % and temperature: (21 ± 3) °C.

Both methods are intended to simulate different handling scenarios: dropping and mixing for the RD method and loading of trucks by a conveyor belt for the CD method. The methods also differ with respect to the intensity and the duration of treatment of the powdered material.

To accelerate the ability to perform risk and /or exposure assessments for nanomaterials, it is evident that nanomaterial-specific dustiness data is an important parameter [6]. From the studies published these last fifteen years on the issue of occupational exposure to nano-objects, their aggregates and agglomerates >100nm (NOAA), the importance of having multi-metric approach for comprehensive exposure assessment is obvious. It means that, in addition to the mass metric, the number and surface area metric as well as the particle size-distributions and offline characterization for physico-chemical characterization should be considered

In that context, both of the EN 15051 methods have been adapted and tested for nanomaterials (i.e. the rotating drum [16, 17]) and the continuous drop systems [18]). The work done within EU projects [6] related (1) to design sampling lines adapted to the aerosol measurement using time resolved techniques like for counting airborne particles as well as for determining size distributions, (2) to develop protocols and (3) to test this on powder nanomaterials composed of nanoparticles of different chemical natures, surface coatings, primary particle sizes and shapes.

Also new dustiness approaches have been developed and tested over the last ten years, for which the motivation were [6]:

- to enable testing of much smaller amounts (from few tens of milligrams to grams) of nanomaterials that are either potentially very toxic and/or costly;
- to develop smaller setups that can be used in ventilated enclosures or fume hoods;
- to establish setups that are easy, simple, and compact to be used by a larger number of laboratories and industries;
- to establish methods that potentially describe different (including worst-case) scenarios in a workplace from those claimed by the RD and CD methods.
- to define new relevant dustiness indices as well as information on size distribution and morphology, which are important elements to consider in risk assessments

Among the dustiness methods, for which a large amount of experimental work has already been performed and tested with a significant number of powder nanomaterials, there are:

- The **small rotating drum** (SRD) method which is in principle a miniaturized version of the rotating drum (RD) [10]. The total volume (5.93 L) of the SRD approximately corresponds to 1/7 of RD (40 L). The cylindrical part of the SRD contains three lifter vanes 120° apart, used to lift and drop the powder during the dustiness test. The airflow (11 l/min) and the inner diameter of the cylindrical part (16.3 cm) were chosen so that the horizontal current of air was equal to the one of the RD method (i.e. ≈ 0.9 cm/s). In addition, the rotation speed of the SRD (11 rpm) was chosen so that the powder sample is lifted and dropped the same number of times (32) than for the RD method, which rotates at 4 rpm and contains eight vanes. The measurement part includes real-time instruments and sampling devices for gravimetric analysis.
- The **vortex shaker** (VS) method is a completely new method with regard to standard dustiness testing and several different configurations of this method have been proposed over time. It comes from an original concept developed as part of a field study devoted to evaluate the aerosol release during the handling of single walled carbon nanotubes (SWCNT) [19]. The VS concept was further developed and tested with different nanomaterial powders, including carbon materials (nanotubes and fullerenes) and metal oxides, but different configurations were carried out due to a lack of harmonization [20-23]. In the configuration that is about to be proposed for standardization at European level, the VS consists of specially designed stainless steel cylindrical tube with a conical bottom (volume of 102 cm^3) that is continuously shaken according to a circular orbital motion (displacement amplitude of 4 mm, rotation speed of 1850 rpm), and in which a small volume (0.5 cm^3) of the test powdered nanomaterial is placed [20]. The emitted aerosol during the vibration is drawn from the outlet tube to the real-time instruments and sampling devices at a total flowrate of 8.4 l/min according to the respirable fraction for gravimetric analysis and for electron microscopy (EM) observation / analysis
- The **Vibrofluidization** (VF) method is based on the use of specially designed vibrating fluidized bed where the mechanical vibration is characterized by a vertical shaking displacement whose amplitude and frequency are in the range 0.059 mm to 9.2 mm and 10 Hz to 300 Hz, respectively [25]. The test sample is positioned on a sintered metal frit held in a metal cylinder which is traversed by a low flowrate of HEPA-filtered air speed from 0.03 to about 0.1 cm/s at the level of the bed. The emitted aerosol is drawn to the measurement part through an equalization tank. The measurement part includes real-time instruments and sampling devices for electron microscopy (EM) observation / analysis.
- The **Venturi** (V) method is based on the use of the Venturi effect to aerosolize a small amount (5 mg) of the test powdered nanomaterial into a 5.7 liter glass jar during a short time of injection (1.5 s). The design of the venturi nozzle results in an air flow velocity of about 70 m/s. The emitted aerosol is drawn from the jar from two sampling ports totaling a flowrate of 6.2 l/min. To improve the sensitivity of the method, an individual test consists of two consecutive 5 mg dispersions (totaling 10 mg of powder dispersed for each test. Originally developed to evaluate the dustiness of pharmaceutical powders [26], this method has been now extended to powdered nanomaterials by NIOSH [27]. In this latter study, the measurement part includes sampling devices (cyclone for respirable fraction and metallic cassette for total fraction) and a size-resolved real-time instrument.

More recently, other methods have been proposed like the one that couples a fluidized bed and a de-agglomeration orifice [28] or another one that includes a magnetic stirrer in a pressurized beaker coupled with a de-agglomeration orifice [29]. These two methods have been used so far with only a very few variety of powdered nanomaterials [30]. The question arises whether these methods belong to the category of the "dustiness" methods. Indeed, the intent behind dustiness testing is that the energy supplied should not be enough to divide the primary particles within aggregates, but liberate some fraction of the loosely bound preexisting primary particles and agglomerates from the powder [27].

Results generated in previous EU projects NANODEVICE and NANOGENOTOX, suggest that the SRD and the VS method may be applicable for assessment of dustiness of nanomaterial simulating fundamentally different work processes. Within NANOGENOTOX, all dustiness data have been incorporated in a series of JRC documents on the characterization and physical properties of amorphous silicon dioxide [31], titanium dioxide [32] and multi-walled carbon nanotubes (MWCNT) [33]. These two projects as well as other (like NANOCARE [34]) also suggest that the absence of a harmonized approach concerning the operation procedures, the measurement strategies and techniques, metrics and size ranges and the procedures of data analysis and reporting limits the comparison of the different dustiness methods, including the RD or CD. Moreover, if there is indeed a recent technical specification document developed at the ISO level [35], there are no standards yet, especially at European level. In this context, the European Commission issued to CEN, CENELEC and ETSI for standardization activities regarding nanotechnologies and nanomaterials a mandate (numbered 461) in which one of the topics to be addressed is the dustiness of bulk nanomaterials [36]. In that context, a pre-normative CEN project (Dustinano) has been launched which objectives are: (1) to develop a harmonized approach for evaluating dustiness for bulk nanomaterials taking into account the different existing concepts and test apparatus; (2) to assess the comparability and the repeatability for a given test system using the developed approaches. Therefore, the present work performed within NanoREG on the VS and SRD methods has benefited greatly from the experimental work carried out in previous projects [31-33], and carried out in parallel within the pre-normative CEN project [37]. In terms of the CEN project output products, five standards are currently being elaborated on the issue of the dustiness of bulk material that may release airborne particles consisting of nano-objects and their aggregates and agglomerates (airborne NOAA).

The expected widespread use of carbon nanotube (CNT)-composites in industrial and commercial applications across industries calls for an assessment of the possible release and exposure to workers [4, 38]. Release of airborne particles containing CNTs may occur at all steps in the life cycle of products, but to date limited information is available about release from actual industrial CNT powders, products and articles containing CNTs. Among the published studies, three of them have used the VS method (but in a different configuration to the one presented here) and with a limited number of CNTs [20 -23]. To our knowledge no dustiness data are available so far with the SRD method [6].

They were two objectives to this experimental study with NANOREG:

- To develop further the Vortex Shaker (VS) and Small Rotating Drum (SRD) dustiness methods, two methods that have been the focus of attention for few years in various EU projects, including an on-going standardization CEN project.

- To develop a new method, referred to as the Vibrofluidization (VF) method.

These developments were to apply within the framework of the NanoREG project to the case of CNTs.

2.3 Description of the work carried out

Dustiness measurements were completed for this deliverable using three different methods; namely the Vortex shaker (VS) method, the small rotating drum (SRD) method and the Vibrofluidization (VF) method. The Table 1 below shows which institute was involved in what method.

Table 1: Dustiness method and institute involved.

Dustiness Method	Vortex shaker (VS)	Small rotating drum (SRD)	Vibrofluidization (VF)
Institute (partner#)	INRS (21)	NRCWE (3)	BAuA (4)

At this stage, it is interesting to note that the three institutes involved have already many years of experience in the methods (dustiness, aerosol measurement) they have used, so that the results presented in this report can be described with a certain level of robustness.

The candidate CNTs have been supplied by the European Commission's Joint Research Centre (JRC) who established a repository of Representative Test Materials (RTMs) that hosts industrially manufactured nanomaterials that are distributed worldwide for safety testing of nanomaterials [39]. CNTs have been received in vials containing each about 100 mg of CNTs. Depending of the bulk density, one or more vials have been used for each experiment. However, due to the subsampling procedure from a single batch by the JRC, the vials provided can be considered to be identical.

The Table 2 lists the carbon nanotubes available for the NanoREG and the ones used by the three involved institutes to perform dustiness measurement.

The core multi-walled carbon nanotubes (MWCNT) NM400 and NM 401 have been tested by the three institutes.

The core single-walled carbon nanotube (SWCNT) NM 46000a has been tested by INRS and NRCWE.

Among the alternatives MWCNT, 10 have been tested by INRS.

Table 2: List of the carbon nanotubes available from NanoREG and for which experiments have been performed.

#	Carbon nanotube			CNT tested by partner (#)		
	Type	Code	MW or SW	NRCWE (3)	BAuA (4)	INRS (21)
1	Core	NM 400	MW	X	X	X
2		NM 401		X	X	X
3		NM 46000a	SW	X		X
4	Alternative	NM 402	MW			X
5		NM 403				X
6		NM 40001a				X
7		NM 40002a				X
8		NM 40003a				X
9		NM 40004a				X
10		NM 40005a				X
11		NM 40006a				X
12		NM 40007a				X
13		NM 40008a				X
14		NM 40009a				X
15		NM 40010a				
16		NRCWE 007				

2.3.1 *Vortex Shaker (VS) method*

The core of the Vortex Shaker (VS) method described in the following sections is in agreement with the proposed standard method that is currently being developed within CEN / TC137 / WG3 as part of the 461 mandate [36].

2.3.1.1 Description of the test system

The core of the set-up consists of a specially designed stainless steel cylindrical tube with a conical bottom that is continuously shaken according to a circular orbital motion (displacement amplitude 4 mm, rotation speed 1850 rpm), and in which a small volume (0.5 cm^3) of the test nanomaterial is placed.

The cylindrical tube with the conical bottom has an interior volume of 102 cm^3. The cylindrical part of the tube has an internal diameter of 3.1 cm and is 13 cm long. The conical part has a base diameter of 3.1 cm and a height of 1.5 cm. A cap is screwed onto the tube which has an inlet for HEPA filtered air, controlled at 50 % RH, and an outlet tube through which the emitted aerosols are transferred to the measuring and sampling instruments. The inner diameter of the inlet and outlet tubes is 9.7 mm and both tubes have a curvature diameter of 34 mm, and are arranged at 180° from one another. The inlet tube enters the cylindrical tube to a length of 12.3 cm. The cylindrical tube and the cap, which both are made of stainless steel, have a total mass of 720 g. The entire system is electrically grounded.

HEPA filtered air passes through the cylindrical tube at a flow-rate Q_{VS} = 8,4 l/min in order to transfer the released aerosol inside the tube to the sampling and measurement section as shown on Figure 1. That corresponds to an air exchange rate of about 86 min^{-1}.

The ejection velocity of HEPA filtered air in the cylinder is 1.9 m/s.

In a recent study [40], it has been demonstrated that the release of airborne particles during dustiness tests can be strongly affected by the humidity of the powder during the storing. Therefore, air in the set-up is controlled for humidity, but not for temperature as this parameter should have a minor effect on the release of particles. The requirement of the EN15051-1 [1] in terms of relative humidity of the air (RH = 50 ± 10 %) was respected. The requirement concerning the temperature within the standard to which the test should be performed is 21 ± 3 °C.

The emitted aerosol during the vibration is drawn from the outlet tube to the real-time instruments and sampling devices through a first flow splitter, which divides the aerosol flow into two flows to two identical respirable cyclones (GK 2.69, BGI) operating at Q_C = 4.2 l/min.

One of the two respirable cyclones is equipped with a cassette with a pre-weighed filter for gravimetric analysis. The sampled particle mass is used to determine the respirable mass dustiness index (see 2.3.1.3). The second respirable cyclone acts as a particle selector (respirable fraction) of the real-time instruments and the TEM grid sampler positioned downstream.

Given the short sampling time (a few seconds in this work), the use of a TEM grid sample necessarily requires a by-pass system (equipped with a 25-mm filter cassette) shown in Figure 1 in order to keep a constant flow through the respirable selector.

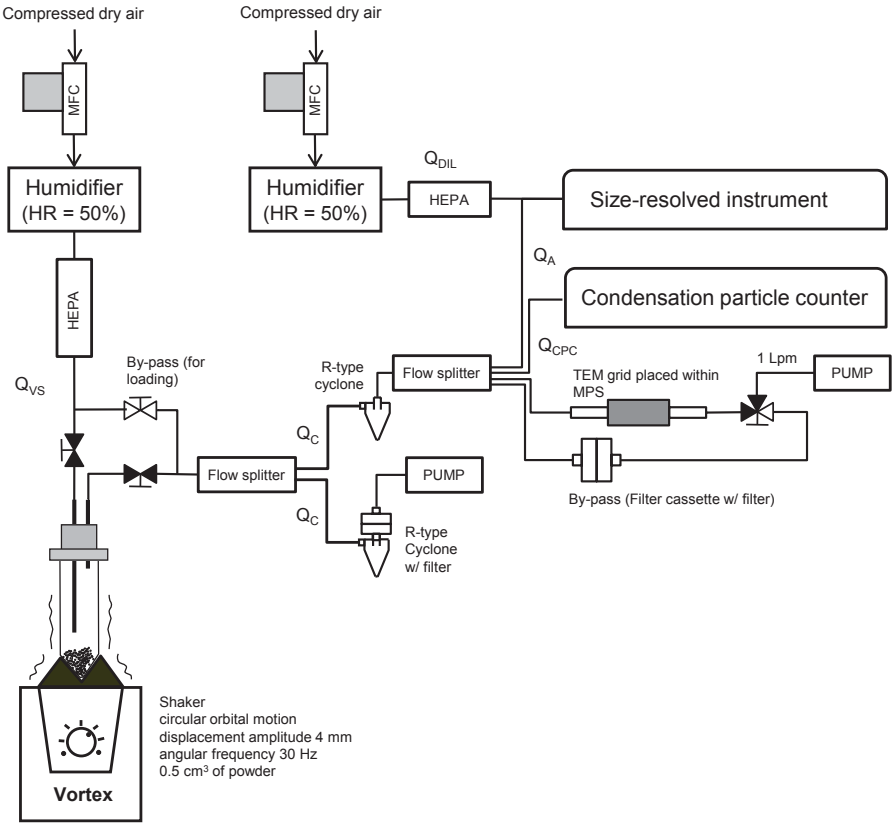

Figure 1: Experimental set-up of the vortex shaker method for determining the number and mass based dustiness index, for characterizing particle-size distribution of the emitted aerosol, and for collecting airborne particles for subsequent EM observations.

The Electrical Low Pressure Impactor (ELPI™, Dekati Ltd) was used as a size-resolved instrument. Because of its wide particle size range (30 nm – 10 µm) and time resolution (~1 s), the ELPI™ has been considered an ideal measurement instrument for the determination of the number-based size distribution over the duration of the test. To prevent particle bounce, overloading and charge transfer during the measurement, sintered plates have been used on all stages. On each plate, about 2 droplets (20 µl of oil, SOGEVAC GS 32) were used.

As a reference instrument for counting particles, a condensation particle counter CPC 3007 (TSI Inc.) was used. This CPC detects particles over the size range of 0.01 to above 1.0 µm (in equivalent mobility diameter) and measures concentrations within the range 0 up to 10^5 cm^{-3} in single count mode.

To collect airborne particles for subsequent observations and analysis by electron microscopy a MiniParticle Sampler (MPS, Ecomesure, France) was used. The MPS is simply a TEM-grid holder that can be used together with Holey Carbon Film TEM grids (400 Mesh, Agar Scientific). The MPS was operated at a flowrate of 1 l/min. Preliminary tests have allowed us to estimate that, given the level of concentration achieved, the sampling time must be of few seconds to achieve sufficient sample loading to allow efficient observation / analysis, while avoiding particle overloading. It was decided to apply a sampling time of 10 s to all CNTs. Given this short sampling time a by-pass system equipped with 25-mm filter holder cassette has been established as shown in Figure 1.

Figure 2 shows a view of two stainless steel cylindrical tubes as well as one positioned in the text bench on the vortex shaker. The entire test bench is located in an approved ventilated enclosure specially designed for handling powders safely (LEV systems, Safetech) to prevent exposure of the operator as shown in Figure 3.

Carbon impregnated conductive flexible tubing have been used to connect the different parts of the set-up as well as the instruments.

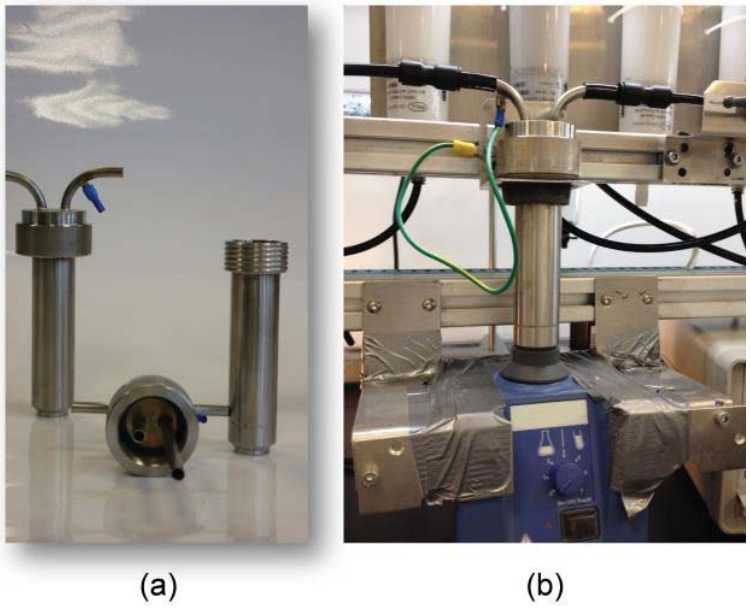

Figure 2: View of two stainless steel cylindrical tubes (a) and one positioned in test bench on the vortex shaker (b).

Figure 3: Full view of the vortex shaker test bench positioned in specially designed ventilated enclosure.

2.3.1.2 Test protocol

The test protocol used in this work is described in the flow chart of Figure 4.

The weighing of the test samples was performed with a XP205 analytical balance (10 µg readability, Mettler Toledo) while the weighing of the 37-mm filters from the respirable sampler was performed with a MX5 microbalance (1 µg readability, Mettler Toledo). The filters used in this study are PVC membrane filters with a pore size of 5 µm (GLA 5000, SKC Inc.). They were chosen because of their low tare weight and moisture pickup for gravimetric stability.

Test samples with a volume of about 0.5 cm^3 were prepared from the sample vials received from the JRC and weighed to the nearest 10 µg. It represents approximately 0.5 % of the volume of the cylindrical tube.

1.5 mL Eppendorf® microtubes were used as containers to prepare the test samples, as shown in Figure 5.

It is recognized that humidity or moisture content of powders can affect their dustiness [34], so controlling for such effects was taken into account in this work. This was achieved by exposing the test samples for at least 24 h prior to the test in a laboratory made humidity-controlled chamber.

Few minutes before the dustiness test is performed, the microtube is closed and transported into the laboratory fume hood where the set-up is located.

Particular attention was given to the cleaning prior to any tests. All pipes and other connections were systematically cleaned, or eventually changed. The checking of the airflows was performed using a primary flow bubble calibrator (Gillian® Gillibrator 2). Prior to each test, the cleanliness of the air was assessed on the basis of measurements made using the CNC. In the case of a non-compliant result, everything was taken from the beginning of the protocol.

During cleaning operations of the test bench and given the fact that the containment barrier of the ventilated enclosure is no longer assured, the operator always wears a powered respirator (3M™ Versaflo™ system), protective gloves with sleeves and a cotton Lab coat, as shown in the Figure 6.

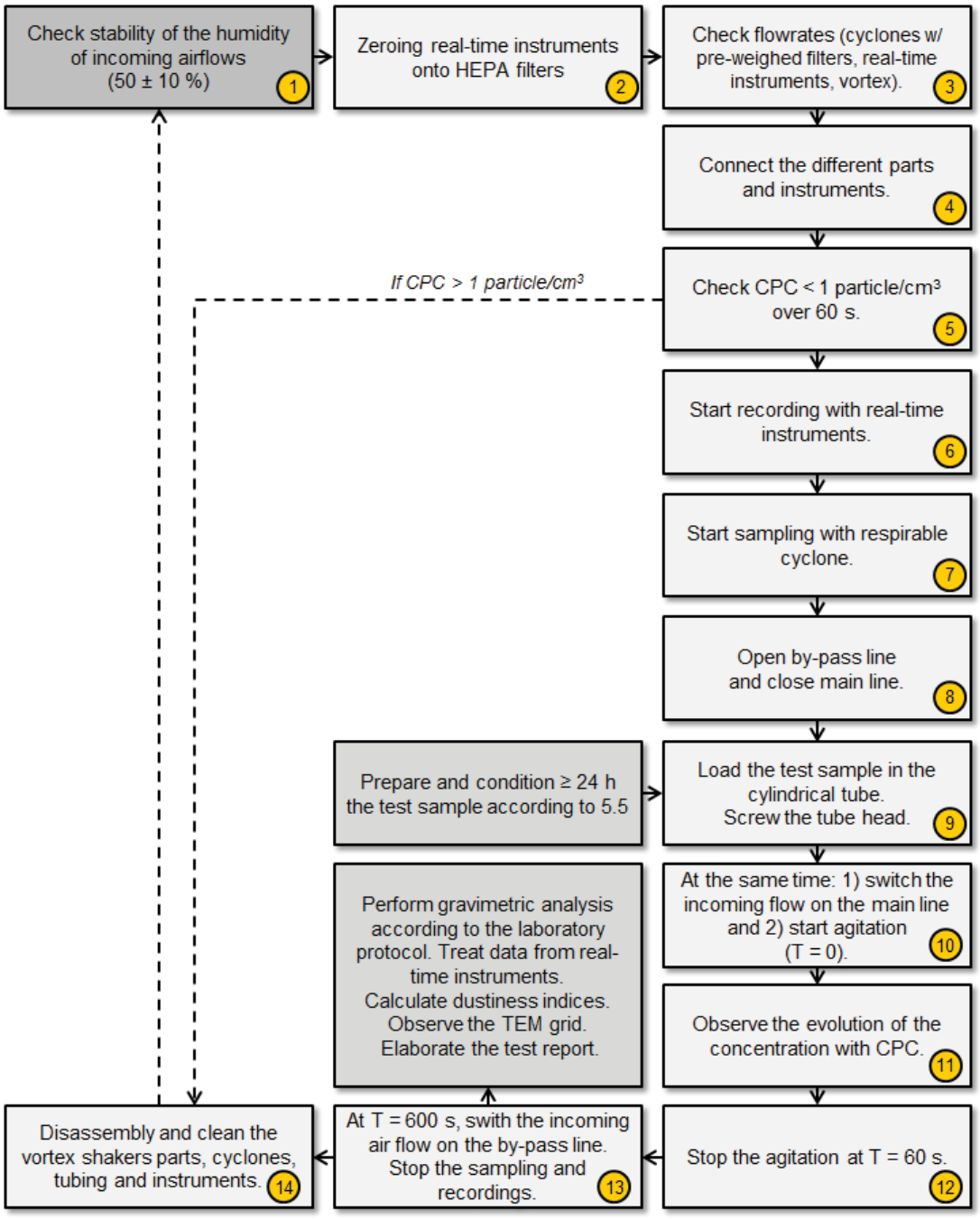

Figure 4: Flow diagram describing the different stages of the test protocol used by INRS.

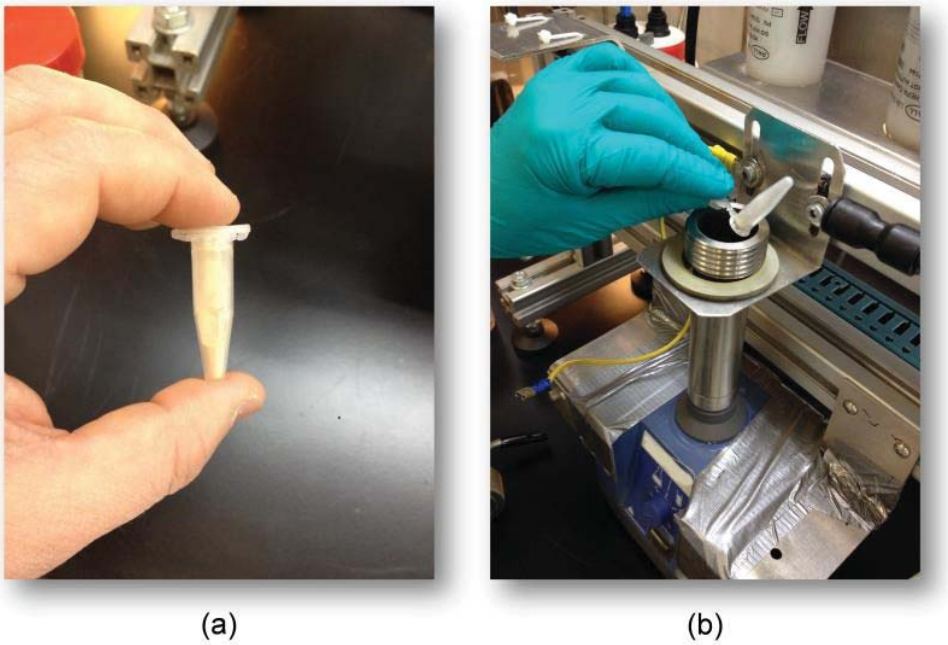

Figure 5: Eppendorf microtubes used as container for the test sample (a) and pouring of the test sample in the cylindrical tube.

Figure 6: Personal equipment used by the operator while cleaning a test bench after a dustiness test.

2.3.1.3 Evaluation of the data

In a first step, the mass of the test sample M_0 and the bulk density of the test sample ρ_{Sample} are determined.

The mass of the test sample M_0 (in mg) is obtained as the difference between the weights of the 1.5 mL Eppendorf microtube once filled with the 0.5 cm^3 of powder and once emptied after the pouring into the cylindrical tube.

$$M_0 = m_{E,0} - m_{E,1}$$

Where M_0 is the mass of the test sample, in milligrams (mg)

$m_{E,0}$ is the mass of the microtube filled with the 0.5 cm^3 of powder, in milligrams (mg)

$m_{E,1}$ is the mass of the microtube emptied after the transfer of the powder into the cylindridrical tube, in milligrams (mg)

The bulk density of the test sample ρ_{Sample} is obtained according to the following equation:

$$\rho_{Sample} = \left(m_{E,0} - m_{E,2}\right)/V_E$$

Where ρ_{Sample} is the bulk density of the test sample, in g/cm^3

$m_{E,2}$ is the mass of the clean microtube, in milligrams (mg)

V_E is the volume of the test sample used, that is 0.5 cm^3

In a second step, the data for the vortex shaker method have been evaluated through three parameters:

- The mass-based dustiness index in the respirable fraction, $DI_{M,R,VS}$ in mg/kg.
- The number-based dustiness index in the respirable fraction, $DI_{N,R,VS}$ in 1/mg.
- The number-based emission rate in the respirable fraction, $ER_{N,R,VS}$ in 1/(mg.s)

The mass-based dustiness index in the respirable fraction, given in milligrams of aerosol per kilogram of powder, was calculated by dividing the mass collected from the respirable fraction (cyclone), in milligrams, by the mass M_0, in milligrams, of the powder placed in the test apparatus using the formula:

$$DI_{M,R,VS} = \frac{\Delta m_f}{M_0} \cdot \frac{Q_{VS}}{Q_C} \cdot 10^6$$

Where:

- $DI_{M,R,VS}$ is the mass-based dustiness index in respirable fraction obtained with the vortex shaker method, in mg/kg.
- Δm_f is the mass collected by the filter in the respirable cyclone, in mg.
- Q_{VS} is the flowrate within the cylindrical tube during the test, in l/min.
- Q_C is the flowrate within the cyclone during the test, in l/min.

The number-based dustiness index in respirable fraction, given in particles per milligrams, was calculated by dividing the number of particles emitted over the duration of the vibration period (60 s), in particles, by the mass M_0, in milligrams, of the powder placed in the test apparatus using the formula:

$$DI_{N,R,VS} = \frac{1}{M_0} \cdot \sum_0^T C_{CPC}(t) \cdot Q_{VS} \cdot \Delta t_{CPC} \cdot \frac{10^3}{60}$$

Where:

- $DI_{N,R,VS}$ is the number-based dustiness index in respirable fraction obtained with the vortex shaker method, in particules/mg .
- $C_{CPC}(t)$ is the number concentration given by the CPC at time t, in particles per cm^3.
- Δt_{CPC} is the time step of the CPC, in s.
- Q_{VS} is the flowrate within the cylindrical tube during the test, in l/min.
- T is the duration of the vibration (60 s).

The number-based emission rate in respirable fraction, given in particles per milligrams per second, is calculated by dividing the number of particles emitted per second over the vibration period, in particles per second, by the mass M_0, in milligrams, of the powder placed in the test apparatus using the formula:

$$ER_{N,R,VS} = \frac{1}{M_0} \cdot \sum_0^T C_{CPC}(t) \cdot Q_{VS} \cdot \frac{10^3}{60}$$

Where $ER_{N,R,VS}$ is the number-based emission rate in respirable fraction obtained with the vortex shaker method, in 1/(mg.s).

In a last step of the data evaluation, the number-weighted size distribution "accumulated" over the duration of the vibration (60 s) is determined from ELPI data. The number-weighted particle size distribution is expressed according to the following formula:

$$f_n(d_i) = \frac{n_{i,VS}}{n_{Tot,VS}} \cdot \frac{1}{\Delta lndp}$$

Where:

- $n_{i,VS}$ is the number of particles emitted over the duration of the vibration, in particles
- $n_{Tot,VS}$ total number of particles obtained from all stages of the the real-time instrument measurement and "accumulated" over the duration of the vibration, in particles

$$n_{i,VS} = \sum_0^T C_i(t) \cdot \frac{Q_{DIL} + Q_A}{Q_A} \cdot Q_{VS} \cdot \Delta t_I$$

$$n_{Tot,VS} = \sum_{all\ stages} n_{i,VS}$$

The number-weighted size distribution $f_n(d_i)$ is plotted versus the equivalent aerodynamic diameter of the airborne particles.

In the ELPI™, once passed the inlet, airborne particles are first charged (by positive ions produced in a Corona discharge) according to their mobility-equivalent diameter and then size classified according to their aerodynamic equivalent diameter in a low-pressure impactor (12 channels in the configuration of the ELPI used in this work). The charged particles collected in each of the insulated impactor stages produce an electrical current recorded by the respective electrometer. The measured current on each channel is converted into number concentration by applying a charging law dependent on mobility-equivalent diameter, it-self related to the aerodynamic diameter [41]. The effective density of the collected particles is required for this conversion. However, the size-dependent effective density (ratio of agglomerate mass to volume) is a parameter which is complex to measure and its experimental characterization is beyond the scope of this work. According to our knowledge, only very few studies have been conducted so far on the determination of the density of carbon nanotubes in aerosol form [42 - 44]. The two studies performed on different MWCNTs indicate that, for one [35], the effective density varies in the range 0.51 to 0.83 g/cm^3 for 0.05 – 0.5 µm mobility size range, while in the second [36] the effective density varied between 0.71 to 0.88 g/cm^3 for 0.1 – 1 µm aerodynamic size range. While the first study shows a size-dependence for the effective density, the second one does not report a specific trend. These two studies have been conducted on different industrial-scale produced MWCNTs in powder form and according to different aerosol generation and characterization methods. Both studies considered quite compact agglomerate structures. The last study [44] reports an effective density of 1.74 g/cm^3 for the condensed phase of the airborne MWCNT, with a method similar to [42]. However, the airborne MWCNTs were generated directly from a gas phase grown carbon nanotubes reactor.

To date, since that knowledge is not yet stabilized and that, moreover, there is no specific effective density data for the nanotubes retained in the NanoREG project, the following assumption was made for the interpretation of data the ELPI in this report: spherical particles with a density equal to the density standard, i.e. 1 g/cm^3. However, for the graphical representation of the size distributions, a density equal to 0.7 g/cm^3 was also used in the calculation from the ELPI raw data. This value of 0.7 corresponds approximately to the mean value obtained by Wang *et al.* [42] and Chen *et al.* [43].

In this work, all currents measured on each channel with the ELPI were first compared to the limit of quantitation (LOQ) of each respective electrometer. If the measured current is less than the respective LOQ, it was not included in the data treatment and converted into number concentration; a value of zero was therefore assigned. The LOQ of each respective electrometer was determined through a specific test carried out separately. This test consists of measuring a particle-free air through a HEPA filter with a previously cleaned ELPI. The HEPA filter is pre-tested with a CPC for leaks and cleanliness, so check that the number concentration downstream of the HEPA filter is zero. A recording of the currents measured by the ELPI through the HEPA filter is performed for about 5 min. These currents correspond to noise signal of the electrometers. The limit of quantification is defined as 10 times the standard deviation of this noise. In this work, the LOQ obtained were in the range from 2.2 to 4.5 fA. This procedure of not considering the currents below a detection limit previously determined, which we call "ELPI LOQ post-processing", allows a good level of confidence in the distributions measurements obtained in the end. To our knowledge, this procedure is hardly performed on the results of ELPI measures or reported in the literature. This approach is particularly essential when the expected concentration levels can be low, which is the case in this work. As a consequence there can be situations where the number-weighted size distribution measured with the ELPI is disregarded due to this ELPI LOQ post-treatment. In this case, we consider it as "ND" which stands for Not Determined.

The electron microscopy observations were conducted at the Laboratoire d'Etudes des Particules Inhalées (LEPI, Paris) in collaboration with INRS. The transmission electron microscope used was a 120 kV JEM-1400 (Jeol) equipped with a CCD camera (ES500 Erlangshen ES500, Gatan Inc.). The JEM-1400 is also equipped with an EDS microanalysis system (Oxford Instruments). Prior to any observation, a size calibration was performed with certified polystyrene latex spheres of 0.88 µm.

2.3.2 *Small Rotating Drum (SRD) method*

The Small Rotating Drum (SRD) method described in the following sections was developed by NRCWE.

2.3.2.1 Description of the test system

The small rotating drum consists of several parts. Figure 7 shows a schematic example over-view of the small rotating drum set-up.

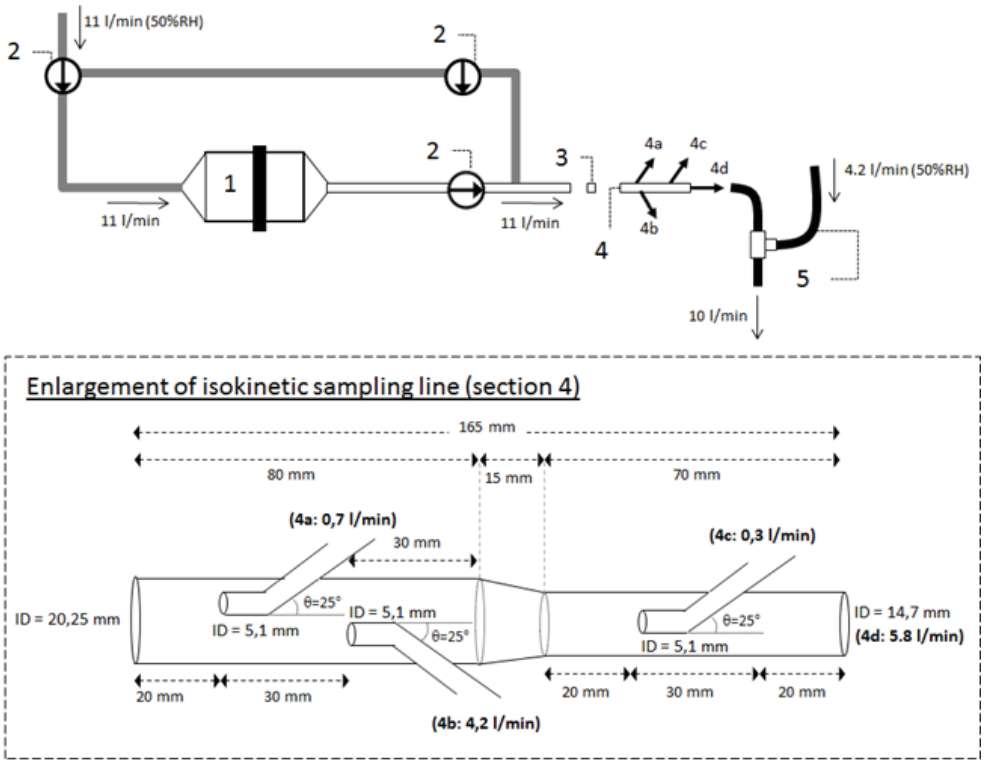

1 Small rotating drum
2 Valves to direct airflow through or bypass the small rotating drum
3 HKI connector (20 mm ID)
4 Sampling line with isokinetic sampling outlets
4a Isokinetic sampling line to condensation particle counter
4b Isokinetic sampling line to respirable cyclone sampler with individual pump
4c Isokinetic samling line to electron microscopy sampler with individual pump
4d Sampling outlet for ELPI
5 Sampling line for measurement with ELPI providing 4,2 l/min make-up air via a T-connector

Figure 7: Sketch of the Small Rotating Drum with sampling train in a configuration where sampling is made using a CPC, a Respirable dust cyclone sampler, a electron microscopy sampler and an ELPI.

The small drum consists of a 23 cm long cylindrical part (r = 8.15 cm) and two 45° truncated conical ends with a center depth of 6.3 cm. These dimensions give a total volume of ca. 5,675 l. The cylindrical part of the drum contains three powder lifter vanes (2 x 22.5 cm) placed 120° apart. The inner surfaces must be polished reaching to reach an arithmetical mean roughness profile of 0.19 µm obtained by vibratory finishing. The drum is rotated driven by a cogwheel belt connected to a programmable electrical engine.

The sampling train is connected to the drum and allows isokinetic (or near-isokinetic) particle sampling of respirable dust, electron microscopy samples, and real-time measurement using the CPC and ELPI aerosol monitoring devices.

A system for humidifying experimental air, capable of delivering 11 l/min through the drum and 4.2 l/min dilution air with highly controlled RH at 50 ± 5 % RH has been used.

According to [5], for testing under standard conditions, the average temperature and the average relative humidity inside the drum shall be 21 ºC (± 3 ºC) and 50 % (± 5 %) respectively and should be stable throughout the entire test period. These conditions are achieved by flushing the drum with the conditioned air without rotating for 5 min as an initial stage of the test. A system for humidifying experimental air, capable of delivering 11 l/min through the drum and 4.2 l/min dilution air with highly controlled RH was therefore used.

Prior to the tests being carried out, the rotating drum is cleaned thoroughly using a suitable vacuum cleaner, wiped with a damp cloth (e.g. isopropanol cloths) and allowed to dry. For test materials that stick to the internal surfaces, it can also be necessary to wash the surfaces with a solution of a detergent in water followed by thorough washing with water, or to clean with a suitable solvent (e.g. propanol).

The inlet stage of the drum is either fitted with a filter capable of filtering most of the laboratory ultrafine particles or an external HEPA pre-filter to the air inlet is used. A background of less than 20 1/cm^3 measured with the CPC is achieved inside the drum when sealed. If not, a check for leakage is performed. The inlet and outlet of the drum are assembled to the appropriate end of the drum.

The outlet of the drum is connected, using an “HKI connecter”, to the “isokinetic sampling train” with instruments, devices and an additional “make-up air” pump (protected by a HEPA filter). The sampling line is attached to the outlet stage of the drum by a rotating coupling device.

The pump, devices and instruments flow rates are checked using air volume flow meters and adjusted if necessary to give a total air flow of 11 l/min through the drum. If added, the volume flows of the make-up air to the relevant instruments are also checked and adjusted as needed.

The instruments are connected to the sampling train using stainless metal or alloy tubes or conductive tubing as illustrated in Figure 7. Bends in tubing are avoided to the extent possible.

2.3.2.2 Test protocol

Because CNT powders and the dustiness index can be sensitive to the relative humidity during storage [40], the test CNT samples have been conditioned at room temperature with 50 ± 5 % RH for at least 12 hours (overnight); before testing.

The test procedure used in this work consists of the following steps:

1. Start the humidified air-flow flow for the test-line and lead it through the bypass tubing. (Follow the instructions for directing the air-flow carefully)
2. Start all real-time monitoring instruments to be used in the test and the pump ensuring the make-up air.
3. Ensure that the test atmosphere is at the correct conditions and recorded.
4. Ensure all instruments are time synchronized to the extent possible and set to log data simultaneously.

5. Start the SRD controller and program it to rotate the drum at 11 revolutions per minute for 60 seconds, if not pre-programmed already. Follow the instructions given for programming the controller.
6. Mount the filter cassette in the respirable dust cyclone; connect all instruments, samplers and make-up air-pump to the sampling line and connect it to the flow-splitter.
7. Zero the mounted drum to position a lifter vane in bottom position.
8. Perform the “zeroing” procedure of the ELPI+. Perform a “blank” measurement with the drum empty and rotating to check the level of “background” particles within the drum. A background of less than 20 1/cm^3 shall be achieved inside the drum when sealed (using a condensation particle counter in the size range of 10 nm to ~1 µm).
9. Disconnect the inlet and outlet sections at both ends of the drum and pull back the slide with the drum and dismount the cone on the inlet side of the drum.
10. Take the test CNT sample; weigh it in; and distribute it along the upwards moving side of the lifter vane placed (vertically) in bottom position by slowly and gently sliding/pouring it out of the weighing boat. The powder should be placed within the central 25 cm of the cylindrical part of the drum (4 cm to the cones at each end). Spread it out along the vane and rather than in a pile. It is important to pour the powder very carefully to avoid loss of dust.
11. Weigh out the weighing boat and record the mass (g) of powder delivered in the drum.
12. Re-assemble the drum, slide the drum carefully back in position mounting position; and connect the inlet and the outlet sections.
13. Ensure that all the data from real-time monitoring instruments are recording by the computers and all data collection run in continuation (set the sampling time for e.g., 12 hours and switch of sampling manually at the end of the test).
14. Change the flow from bypass to test flow leading the humidified air through the drum. (Follow the instructions for directing the air-flow carefully). Changing the air-direction from bypass air to go through the drum is the start of the dustiness test sequence and defines t = 0 sec.
15. Establish test conditions in the drum and sampling train for 5 minutes (300 sec) while the drum is at rest and the powder sample at the bottom of the drum. The 300 sec. period is used to define the “background” air for quantification of the data collected by the real-time monitors.
16. At t = 300 sec, start the pump attached to the respirable dust cyclone + filter cassette and immediately thereafter, start 60 seconds of rotation of the drum at 11 rpm by pressing start on the touch screen of the controller unit. This 60 sec. period defines the rotating drum agitation in the SRD test.
17. After stop of the 60 seconds agitation, allow the real-time instruments and the respirable dust cyclone to collect dust and data for an additional 120 sec. This post-rotation sampling allows collection of the entire dust cloud generated during the test.
18. After 180 s, the test is completed and sampling pumps are switched off.
19. Change the air-flow to bypass position. (Follow the instructions for directing the air-flow carefully).

20. Dismount the filter-cassette from the respirable dust cyclone, place the cassette lit and store the filter-cassette in a lidded box.

In this work, due to amount available, 2 g of CNT was used for NM 400 and NM 46000a. For NM 401, only 0.3 g was used.

2.3.2.3 Evaluation of the data

The mass-based respirable dustiness index ($DI_{M,R,SRD}$) in mg/kg is given by the following equation:

$$DI_{M,R,SRD} = \frac{\Delta m_{filter}}{M_{powder}} \cdot f$$

Where:

- M_{powder} is the mass of the test sample, in kg
- Δm_{filter} is the mass collected by the filter in the respirable cyclone, in mg
- f is the dilution factor, equal to 11/4.2.

The number-based respirable dustiness index ($DI_{N,R,SRD}$) in 1/mg is given by the following equation:

$$DI_{N,R,SRD} = \frac{1}{M_{powder}} \cdot \sum_{0}^{T} C_{CPC}(t) \cdot Q_{SRD} \cdot \Delta t_{CPC} \cdot \frac{10^3}{60}$$

Where:

- $C_{CPC}(t)$ is the number concentration given by the CPC at time t, in particles per cm^3.
- Δt_{CPC} is the time step of the CPC, in s.
- Q_{SRD} is the flowrate within the small rotating drum during the test, in l/min.
- T is the duration of the test (180 s).

2.3.3 *Vibrofluidization (VF) method*

The Vibrofluidization (VF) method described in the following sections is developed by BAuA.

2.3.3.1 Description of the test system

The vibrofluidization-method aims to establish a fluidized state of the powder base material. In a simplified model, a fluidized bed is established when the individual powder grains are exposed to an aerodynamic drag that cancels out gravity but are still bound to the bed by inter-particulate adhesive forces. Such forces can be van-der-Waals or Coulomb, amongst others. In a fluidized bed, the pour density of the powder is reduced and the bed expanded. Since the adhesive forces are weaker at the bed surface and particles undergo chaotic motion, particles can become lose and are transported by the air stream.

Fluidization has different states, the most important of which are the incipient bed and the bubbling bed. Figure 8 shows a simplified depiction of both states of the powder bed: (a) shows the in initial fixed powder bed, (b) the incipient bed and (c) the bubbling bed.

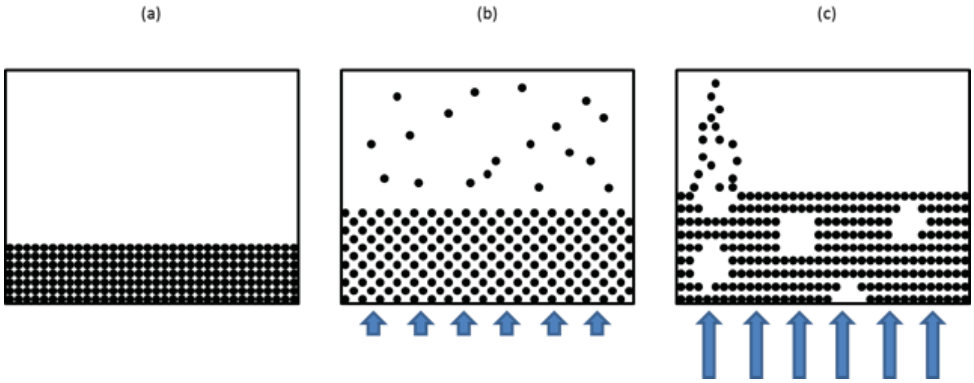

Figure 8: Different states of a powder bed during fluidization: (a) fixed bed – no flow, (b) incipient bed - flow near minimal fluidization velocity, (c) blubbing bed – high flow.

At zero flow or a flow velocity smaller than the so-called minimum fluidization velocity (defined by the minimum drag necessary to overcome gravity), the powder bed is fixed. When the flow is increased over the minimum fluidization velocity, the powder bed expands as the distance between the individual powder grains increases. At the top of the powder bed, some particles are picked up by the flow. At larger flow velocities, bubbles are formed in the powder. Particles are transported by the bubbles and are released when a bubble “bursts” when leaving the powder bed.

For powders with very small grains, e.g. powder of nanomaterials, the traditional method of running a laminar flow through a powder bed usually doesn’t result in a fluidized bed, because the inter-particular forces are not overcome. Also, such powders tend to skip the incipient state and instead of a laminar flow running through the whole bed, small capillaries are formed. The bubbling bed is also not established as it is hard to break up the capillaries just by increasing the velocity of the flow. Instead, new and larger capillaries are formed until a so-called plug flow is formed where the whole powder bed is elevated until it collapses and capillaries are again formed. For this reason, an additional manipulation of the powder bed is necessary to overcome the inter-particular forces. In the VF-method, this is accomplished by vertical vibration of the powder bed. Vibrations effectively disturb the formation of capillaries and facilitate the incipient state. In other words, the minimal flow velocity is decreased. A bubbling bed also can be established.

A vibro-fluidized bed shows bed expansion, with its height dependent on the flow velocity and frequency.

The layout of the experimental setup is shown in Figure 9 (a). It consists of a shaker TIRA (TV 52110) that is connected to the container that retains the sample material, shown in (b).

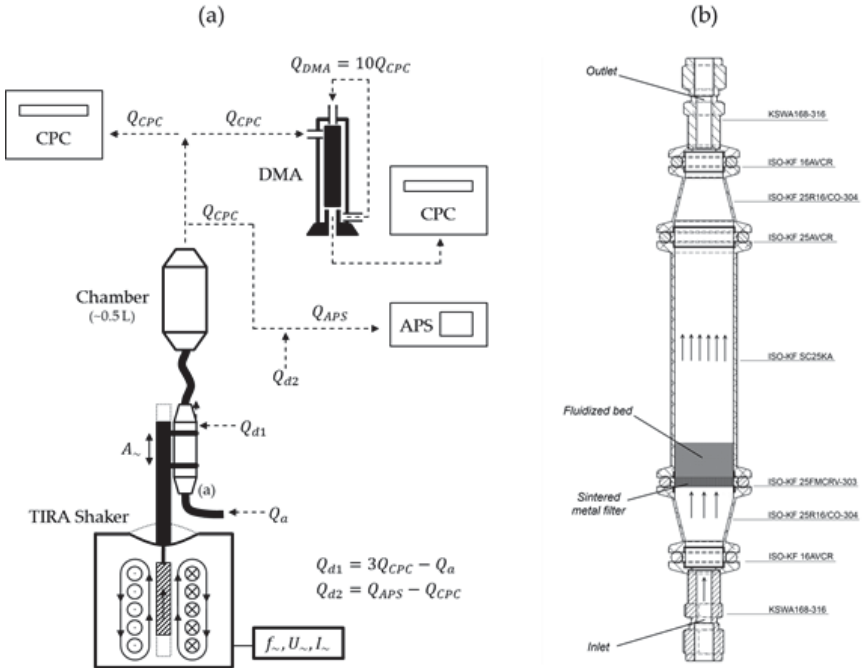

Figure 9: (a) Experimental setup and flow scheme of the dustiness test. Detailed descriptions of both figures are given in the text. (b) Schematic layout of the container that retains the fluidized bed.

The TIRA shaker contains a high-voltage coil that generates an electrical field. A magnet that is situated in the windings is moved in direction of the electrical field. The magnet is mechanically connected to a rubber membrane that transfers the movement to the container. An alternating voltage $U_\sim$ (V) with frequency $f_\sim$ (Hz) and amplitude $I_\sim$ (A) generates an alternating field that sways the magnet with mechanical displacement $A_\sim$ (mm), given by an empirical formula:

$$A_\sim = (4{,}35 \pm 0{,}08) \cdot U_\sim \cdot e^{((-f_\sim)/(14{,}1 \pm 1{,}1))}$$

The constants in this equation change depending on the mass that is moved. The container weight is roughly 600 g.

Compressed air with a sample flow rate Q_a flows through the container and transports particles towards a small equilibrium chamber. Before entering the chamber, a side stream air flow with a flow rate Q_d1 is added for dilution. Dilution was necessary since the measurement instruments require higher flow rates than the sample flow rate. After leaving the chamber, the flow is split for the instruments, which were an Aerosol Particle Sizer (TSI APS 3321), which required a second dilution stage Q_d2, a stand-alone Condensation Particle Counter (Grimm CPC) and a Scanning Mobility Particle Sizer (Grimm SMPS), i.e. a scanning Differential Mobility Sizer (DMA) in series with a CPC.

Figure 9 (b) shows the schematic layout of the container for the sample material in which the vibrating bed is created. The whole assembly is built from vacuum components with ISO-KF standard (see figure for part numbers) and is set up vertically. The inlet air flow enters the assembly through a 16 mm wide entrance and is led through a conically shaped reducer towards a sintered 25 mm wide metal frit (20 µm pore size) before entering a 100 mm long pipe. The purpose of the frit is to allow a continuous laminar pipe flow through the system while keeping the powder bed in place. Particles that are emitted from the powder bed are transported with the air flow towards the outlet. The outlet is symmetrical to the inlet.

2.3.3.2 Test protocol

Sample preparation

The amount of sample material M is determined based on the desired powder bed height x, calculated with:

$$M = \rho_{pour} \cdot V_{bed} = \rho_{pour} \cdot (d/2)^2 \cdot x$$

Where ρ_{pour} is the pour density of the material.

d is the diameter of the frit.

The state of the base material affects the results of a dustiness test. Hence, sample preparation should be performed under well-controlled conditions. Optimally, several samples should be prepared in advance when a series of dustiness tests for the same material is planned. Samples should be stored in metallic containers without exposure to sunlight, if possible in protective gas like argon.

The container is filled with the sample material. The container must be closed and made air-tight before it is mounted in the TIRA shaker.

Preparation of test system

The dustiness test system, i.e. container, chamber and tubing must be cleansed of any remaining particles from the previous dustiness test. Prior to each dustiness test, the system must be rinsed using pressured air. The particle concentration in the chamber is monitored using the CPC and APS. The system is regarded clean when the particle number concentration remains lower than 10 #/cm³ over a sufficient period of time (around 10 minutes).

Before performing dustiness tests with a new material, the system must be cleaned more thoroughly, by disassembling the system and cleaning the parts individually with ethanol.

The test system must be checked for leaks.

The container is firmly mounted on the TIRA shaker, e.g. by using two pipe clamps. It must be ensured that the sample flow is zero when the container is connected to the test system.

The test system as well as the container must be grounded. It is recommended to use conductive tubing.

The function generator for the TIRA shaker is set to the control parameters (frequency, voltage).

Instruments are started during the cleansing of the test system. It must be ensured that the instruments are synchronous, in particular when using different computers for instrument control.

Dustiness test

The dustiness test is started by switching on the TIRA shaker and regulating the flow for the container.

Duration of the dustiness test is 2 hours.

Occasionally, aerosol sampling is performed by exchanging the SMPS with a sampling device working with the same flow rate as the SMPS, e.g. a filter.

2.3.3.3 Evaluation of the data

Particle size distribution < 1000 nm

The SMPS monitors the particle size distribution over the duration of the dustiness test in the size range of 10-1000 nm. Particle size is expressed as the diameter of a sphere with equivalent electrical mobility as the particle.
SMPS measurements over the course of the dustiness test are used mainly to assess if and how many nanoparticles in the size range of 10-1000 nm the powder emits. Size data is plotted but not interpreted, because there are constraints for interpretation of electrical mobility data of nanotubes.
The electrical mobility of a particle depends on particle shape, its alignment relative to the flow streamlines and charge, amongst others. For classification, the charge distribution of an aerosol is set to Boltzmann-equilibrium by a neutralizer (i.e. almost all particles have either +e or –e charge). However, nanotubes are easily polarized and can be aligned with an electrical field. This affects their electrical mobility since the Coulomb force on a nanotube cannot be modeled by the Coulomb force on a point charge, which the conventional definition of electrical mobility assumes (and the measurement software of the SMPS). Therefore, the usual interpretation of mobility equivalent size data for nanotubes, in particular single nanotubes, cannot be regarded as scientifically sound.
Even though, SMPS data is fitted using a lognormal model (with ln-log10 conversion parameter of 2.35):

$$y(x) = y0\ x + \frac{2.35\ A}{\sqrt{2\pi}\log(w)}\mathrm{Exp}\left[-\frac{\left(\log(x) - \log(\tilde{d})\right)^2}{2\ log(w)^2}\right]$$

The fitting parameters where therefore $y0$ (offset), A (amplitude, i.e. total number of particles), w geometric standard deviation) and $\tilde{d}$ mean particle size, electromobility diameter).

Particle size distribution > 1000 nm

The APS monitors the particle size distribution of the aerosol in the range above 1000 nm. In the APS the particle size is described with the aerodynamic diameter, the diameter of a sphere with a density of 1 g/cm³ and equivalent terminal velocity as the particle (velocity caused by gravity).
Similar to the case of electrical mobility, APS data for single nanotubes must be interpreted carefully. The APS uses time-of-flight measurements in which particles pass two light beams to measure their rate of acceleration in a nozzle, which is determined by their aerodynamic size. Single nanotubes in a laminar flow tend to align themselves with the flow streamlines so that their flow cross-sectional area is minimal and hence their aerodynamic diameter.

2.3.3.4 Summary of dustiness profiles

The instrument data is represented as so-called dustiness profiles. Figure 10 shows the layout with example data.

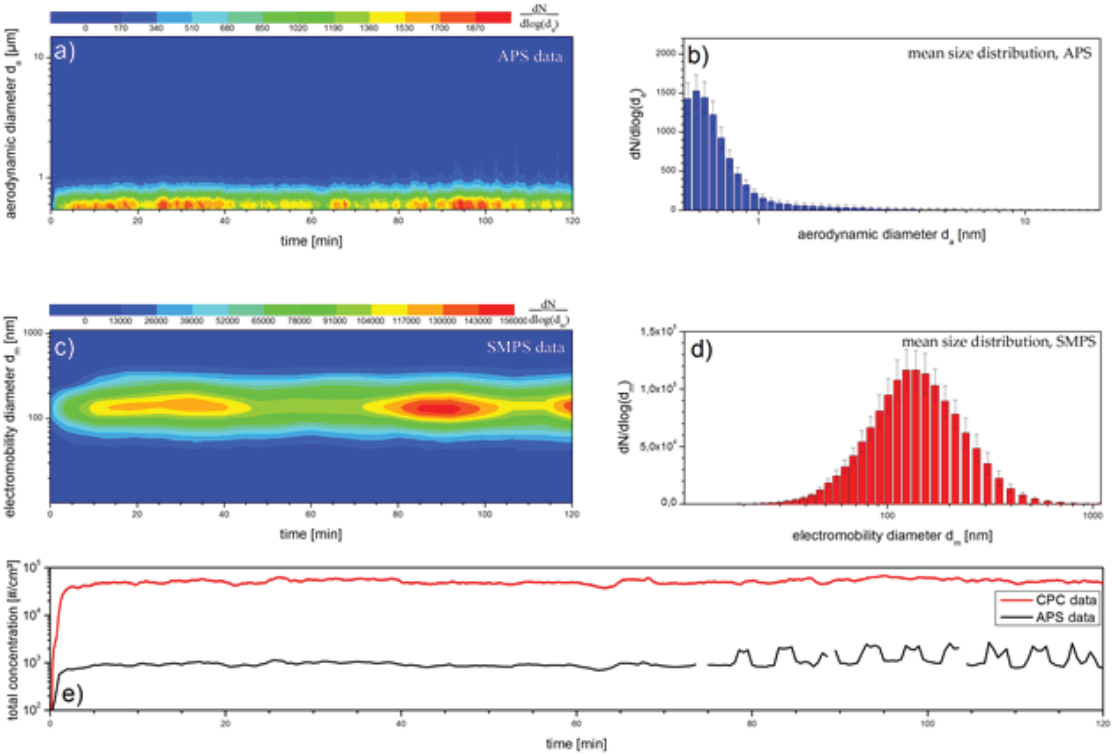

Figure 10: a) Histogram of the particle size distribution measured with the APS; b) Measured mean size distribution over the course of the dustiness test. Accordingly; c) and d) Histograms of the particle size distribution measured with the SMPS and the mean size distribution, respectively; e) Total particle number concentration, measured with the APS and the SMPS as a function of time.

2.3.3.5 Dustiness indices

A number based dustiness index [1/mg] was determined by the ratio of the integral of the particle number concentration over the time of the dustiness test, measured with the CPC, and the initial mass of the base material.

Mass-based dustiness indices are determined by the ratio of the total mass of particles that were emitted over the course of the dustiness test and the initial mass of the base material, in a metric of mg/kg. For single fibers, a material density of ρ_{CNT} = 1.75 g/cm³ is assumed, a value determined by DMA-PMC measurements [43]. The total mass M of single fibers emitted over the course of the dustiness test was determined by:

$$M = N\left(L \times \pi\left(\frac{d_{CNT}}{2}\right)^2\right)\rho_{CNT},$$

Where:

N is the total number of particle that were emitted

L and d_{CNT} are the length and diameter of a single CNT, respectively.

For NM400 and NM401, values for L and d_{CNT} can be taken from their respective JRC material reports. For fiber-like aggregates, their effective density can be used to calculate their mass, when the mobility diameter is known. Effective density is hard to determine without additional measurements using a DMA-PMC or DMA-ELPI setup, not conducted in this work. Therefore, all dustiness indices refer to single fibers emitted during the dust generation. Consequently, CPC data, not APS data, is used to determine indices.

It must be said, that the mass-based dustiness index is defined based on the continuous drop test, in which the whole initial material is transported in a specific time frame, so that a “deployed” mass can be compared to an emitted mass. For a dustiness test like the vibrofluidization method, in which the base material is not transported as a whole, such definition is nonsensical because the emitted mass depends on the time frame in which the test was conducted. The traditional dustiness coefficients are still determined and presented in this deliverable.

2.4 Results

In this chapter the results obtained for the three methods are presented through tables and/or graphs.

2.4.1 *Vortex Shaker (VS) method*

Overall, 42 experiments have been conducted at INRS with the VS method for the 14 nanotubes, as shown in Table 3. This table also shows the average relative humidity (in %) during the conditioning of the test samples and during the dustiness tests itself as well as the average temperature during conditioning. These results indicate that the tests were carried out under the conditions required by EN 15051.

Table 3: Relative humidity and temperature obtained during conditioning and testing.

Number of experiments	Average relative humidity (%) during		Average temperature during conditioning (°C)
	conditioning (24 h)	Dustiness test (600 s)	
42	50.1 ± 0.8	50.9 ± 0.6	22.1 ± 0.3

Figure 11 below shows for each tested CNT the average values of humidity during the conditioning stage and during the dustiness test itself.

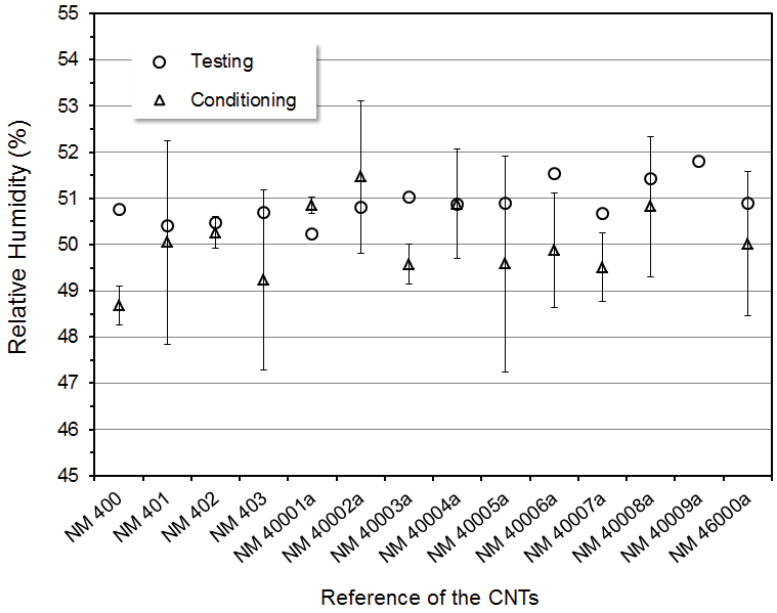

Figure 11: Relative humidity (in %) during the conditioning of the test samples (> 24 h) and during the dustiness testing (600 s) for the nanotubes. The average values for the conditioning are shown their standard deviations.

Figure **12** shows the average masses used for the dustiness tests for each of the 14 CNTs. The masses used range from about 200 mg down to 5 mg. These masses correspond to the volume of 0.5 cm^3 taken as reference volume in the vortex shaker method. The large variations are due to the difference in terms of bulk density of the CNTs.

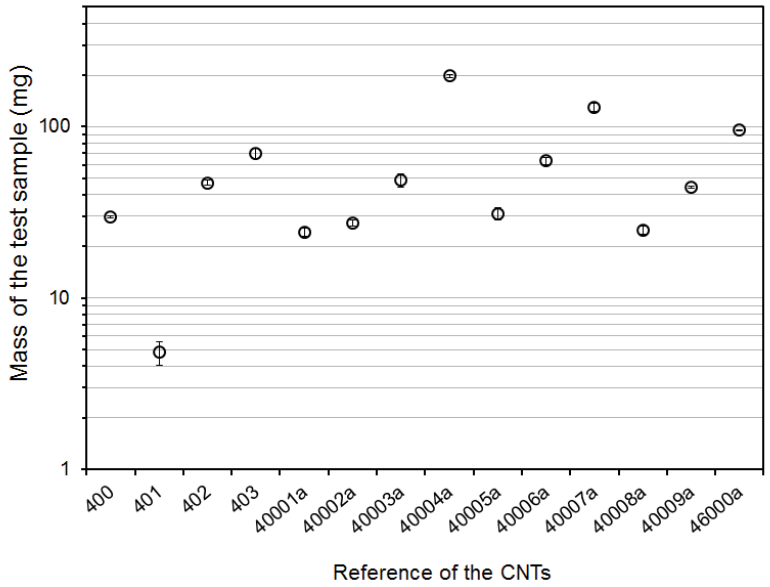

Figure 12: Average masses used for dustiness testing for each of the 14 CNTs tested with the vortex shaker method. Average values are presented with their standard deviation.

Figure 13 shows the bulk density of the 14 CNTs for which dustiness tests have been conducted. The min and max values obtained were 0.01 and 0.4 g/cm^3 respectively. The CNTs powders show great variability in terms of bulk density as the ratio max/min is ~40. It is interesting to note that these values are between 5 and 235 times lower than those of the effective densities which we refer above [35, 36], as well as well below the theoretical graphite density of 2.27 g/cm^3. However, these bulk density values are in accordance to other published effective densities [35]: 0.14 - 0.16 g/cm^3 for Baytubes (BMS, Germany) and 0.22 g/cm^3 for TNM3 (Timesnano, China).

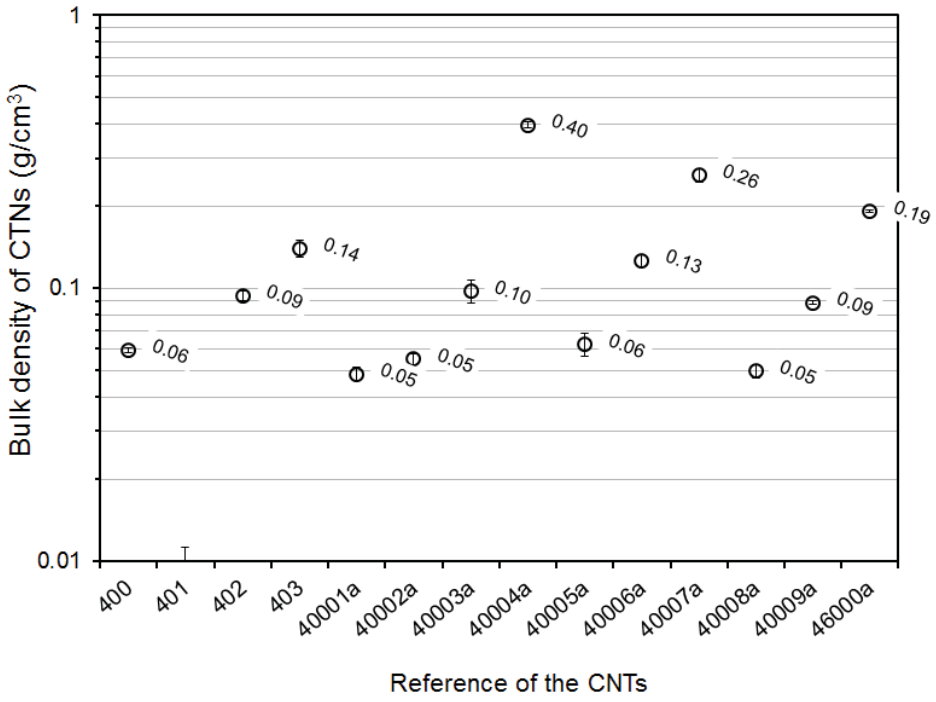

Figure 13: Bulk density of the 14 CNTs tested at INRS. Average data are shown with their 95% confidence intervals.

Figure 14 presents the mass-based dustiness index in respirable fraction, given in milligrams of aerosol per kilogram of powder, for the 14 tested CNTs. On the figure, average values are presented with the 95% confidence intervals. It can be observed that there is good reproducibility between the tests; the average coefficient of variation is 16% with min and max values of 4 and 64 % respectively. On this figure is also presented the limit of detection (LOD) in terms of mg/kg; this corresponds to the ratio of the gravimetric detection limit to the sample mass used for the test. The LOD to be set to the gravimetric analysis of filtered samples was obtained from the quantification of the reproducibility of blank filter weighing. The gravimetric detection limit obtained was 17 µg.

For two of the tested CNTs, the mass-based dustiness index could not be obtained, due to the low mass of CNT emitted and sampled on the filter of the cyclone. These are NM 403 and NM 46000a, which is the SWCNT. For these two, the mass-based dustiness index should be considered lower than the values in red in the figure.

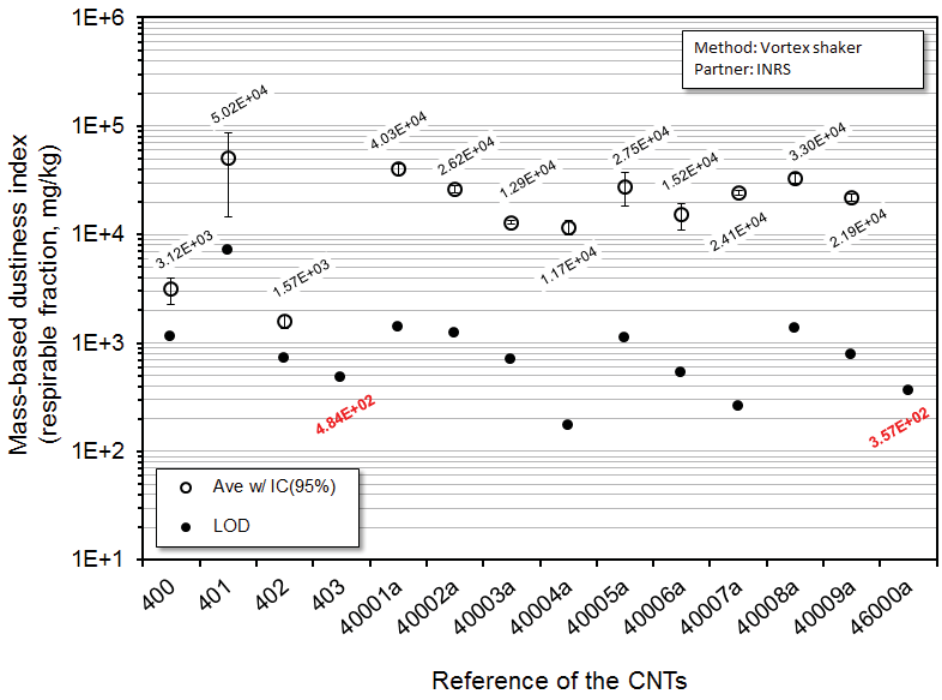

Figure 14: Respirable mass dustiness index (in mg/kg) for the 14 CNTs tested at INRS. Average values (empty circles) are presented with their 95% confidence interval. Black circles correspond to the LOD.

Figure 15 presents the number-based dustiness index in respirable fraction, given in particles per milligrams, for the 14 tested CNTs. In this case also the reproducibility is good since the average is 11% with min and max values of 1% and 29%, respectively. The values cover 2.5 orders of magnitude. MWCNT 40001a corresponds to the highest value and SWCNT 46000a gives the lowest value.

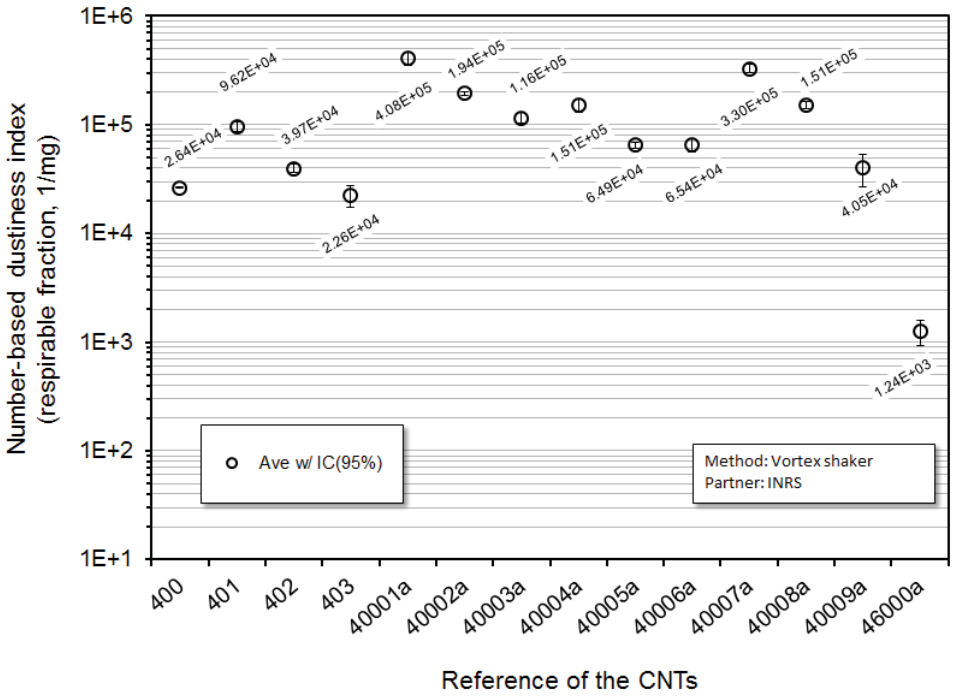

Figure 15: Respirable number dustiness index (in 1/mg) for the 14 CNTs tested at INRS. Average values (empty circles) are presented with their 95% confidence interval

Figure 16 presents the number-based emission rate in respirable fraction over the vibration period (60 s). In this case also the reproducibility is good since the average is 11% with min and max values of 1% and 29%, respectively. As for the number-based dustiness index, the number-based emission rate values cover 2.5 orders of magnitude.

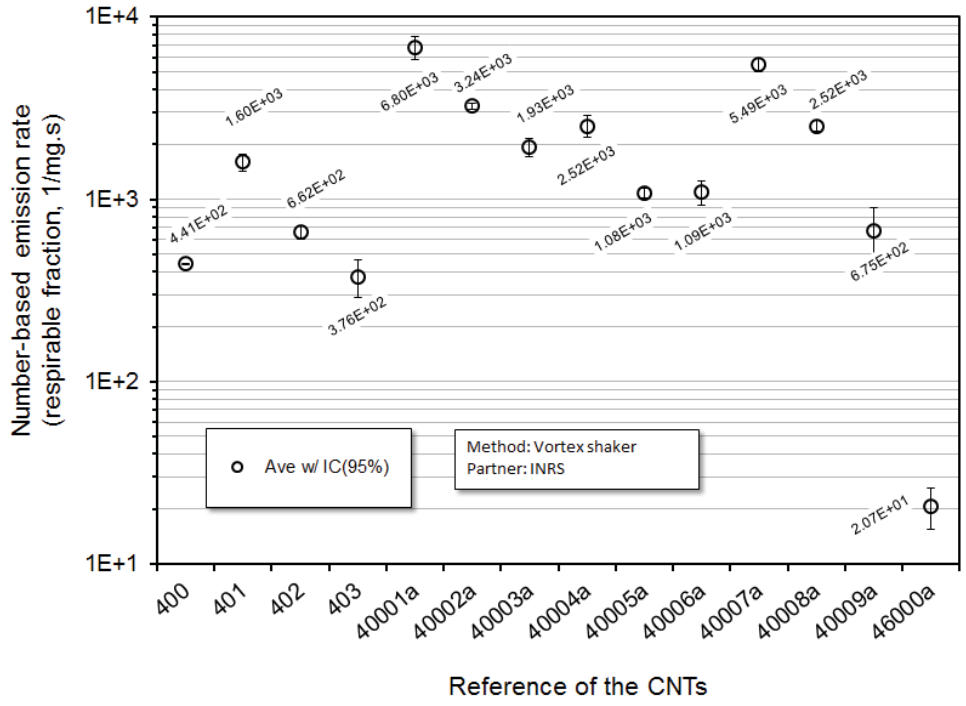

Figure 16: Number-based emission rate (1/mg.s) in respirable fraction over the vibration period (60 s) for the 14 CNTs tested at INRS. Average values (empty circles) obtained on three repeats are presented with their 95% confidence interval.

Figure 17 presents the mass- ($DI_{M,R,VS}$) and number-based ($DI_{N,R,VS}$) dustiness indices in respirable fraction. Average values, and 95% confidence interval are provided. In addition of the two indices, the limit of detection in terms of mass-based dustiness index LOD($DI_{M,R,VS}$) is shown.

Overall, these results demonstrate that the developed protocol leads to accurate dustiness indices. Indeed, the median coefficient of variation (CV) on the $DI_{N,R,VS}$ is 10%, similar to the median CV for the $DI_{M,R,VS}$ (10%).

Another observation concerns the ranking for the different CNTs. In Figure 17 the dustiness data are ranked according to the $DI_{N,R}$ from the highest (NM 40001a) to the lowest (NM 46000a), which is the SWCNT. It can be observed that the ranking show a different order depending on the different dustiness metrics, mass- or number-based. Moreover, no correlation has been found between the two dustiness metrics. This suggests that the choice of a dustiness metric has significant implications for exposure modeling or when comparing powders. This supports the choice made in this work to have developed a dustiness method following a multi-metric approach.

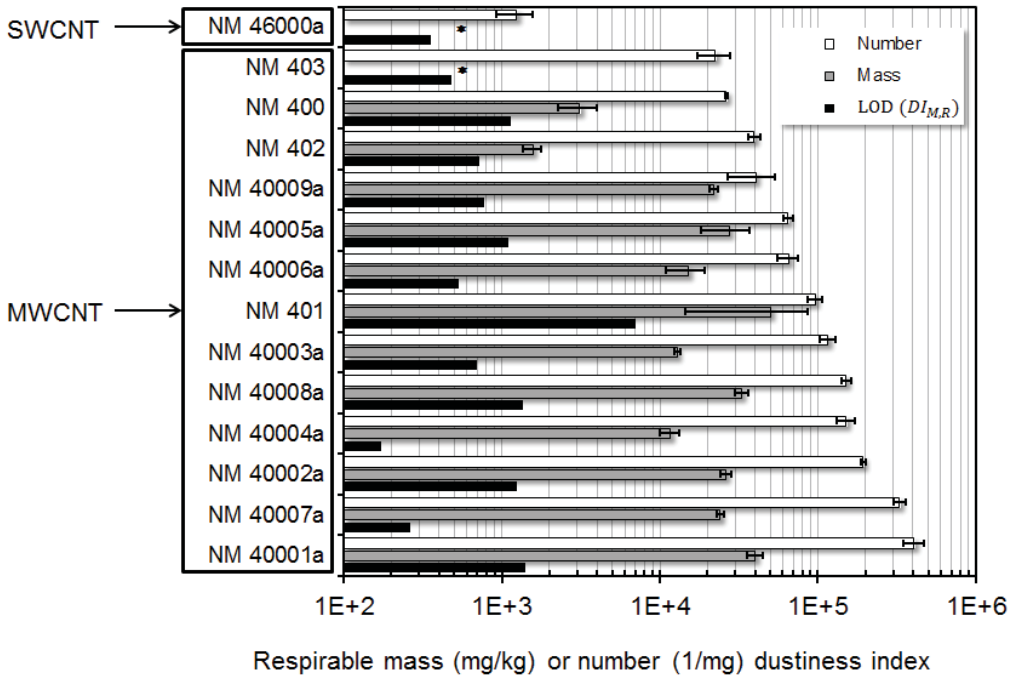

Figure 17: Respirable mass dustiness indices (in mg/kg) and respirable number dustiness indices (in 1/mg) for the fourteen CNTs obtained with the VS method. Average values are presented with their 95% confidence interval. Black bars correspond to the LOD($DI_{M,R}$). Symbol $*$ indicates that the mass dustiness indices obtained were below the LOD($DI_{M,R}$).

Figure 18 presents the number-based emission rate (1/mg.s) in respirable fraction versus time for three of the tested CNT, namely the SWCNT (46000a), the MWCNT 403 and the MWCNT 40007a. This graph illustrates that there are different time profiles of the release of respirable particle number during the rotation period. However, all show a similar pattern with an initial burst followed by a sharp decrease. Although the amount of mechanical energy supplied to the powder sample is the same in the VS method, the duration and level of the initial burst may vary from a CNT to another.

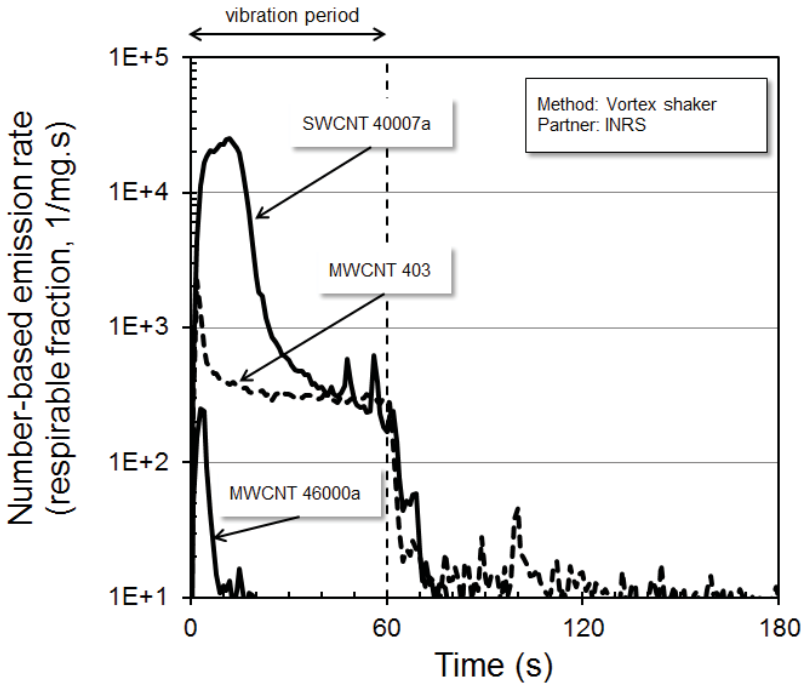

Figure 18: Number-based emission rate (1/mg.s) in respirable fraction versus time for three of the tested CNT.

Figure 19, Figure 20 and Figure 21 show the number-weighted size distributions versus aerodynamic equivalent diameter "accumulated" – or time-integrated – over the period of vibration (60 s) for the CNT 400001a, 40002a and 40009a respectively. In each Figure, the histograms correspond to average values obtained over 3 experiments (one standard deviation) and are calculated from the current distribution for two densities: 1 and 0.7 g/cm^3. A fitting procedure has been applied to obtain a continuous particle size distribution on the histogram that corresponds to the density standard, i.e. 1 g/cm^3. In our approach a bi-modal lognormal distribution was assumed to be an acceptable solution for all cases. These three figures illustrate the type of distributions obtained in this work of the released aerosol: bimodal distribution with one mode in the sub-micrometer range and another mode on the micrometer range, or monomodal distribution with a mode positioned in the micrometer range.

Table 4 presents the results obtained from the fitting procedure on the number-weighted size distributions measured with the ELPI. Only the number of modes and their value in micrometers (µm) are indicated here. Mode 1 stands for the highest mode of the fitted curve and mode 2 for the lowest mode. As explained in paragraph 2.3.1.3, the situations indicated as "Not Determined" are the results of the "ELPI LOQ post-processing" procedure. Over the fourteen CNT tested, only nine number-weighted size distributions could be obtained, and five have been disregarded. It is interesting to note that CNT for which the number-weighted size distribution could not be retained are not always the CNT for which the lower indices (in number or mass) were obtained.

Over the nine size distributions retained, four of them are characterized by a bimodal distribution, and only one among the four shows a Mode 1 in the sub-micrometer range. Moreover, all the five monomodal distributions are characterized by a mode in the micrometer range.

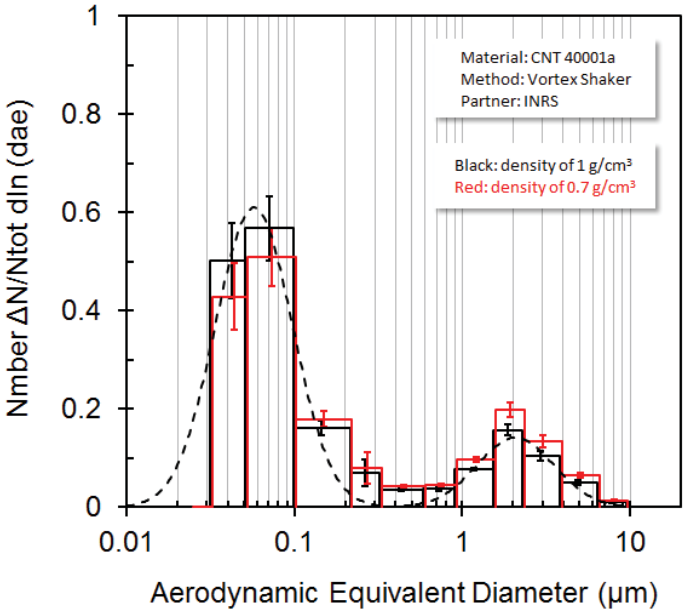

Figure 19: Number-weighted size distribution versus aerodynamic equivalent diameter time-integrated over the period of vibration (60 s) for the CNT 40001a. Histogram is presented for two densities (1 and 0.7 g/cm^3); average values are shown with their standard deviation over 3 experiments. Dotted line corresponds to the fitted distribution obtained for the density of 1 g/cm^3.

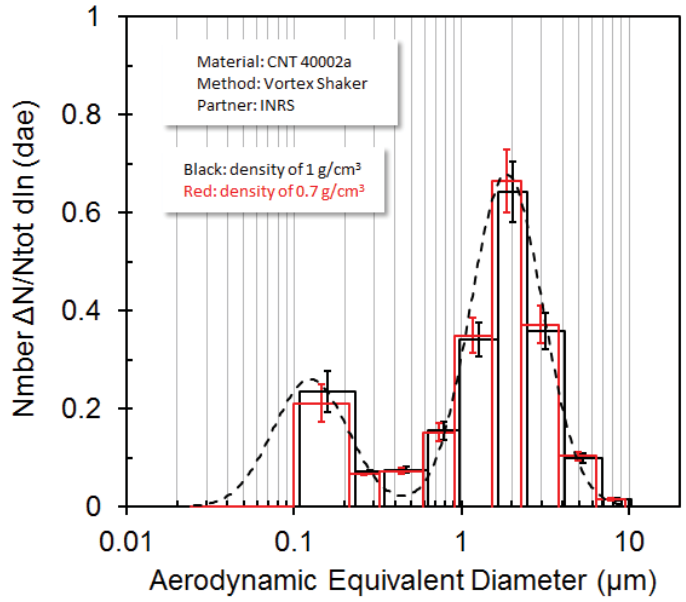

Figure 20: Number-weighted size distribution versus aerodynamic equivalent diameter time-integrated over the period of vibration (60 s) for the CNT 40002a. Histogram is presented for two densities (1 and 0.7 g/cm^3); average values are shown with their standard deviation over 3 experiments. Dotted line corresponds to the fitted distribution obtained for the density of 1 g/cm^3.

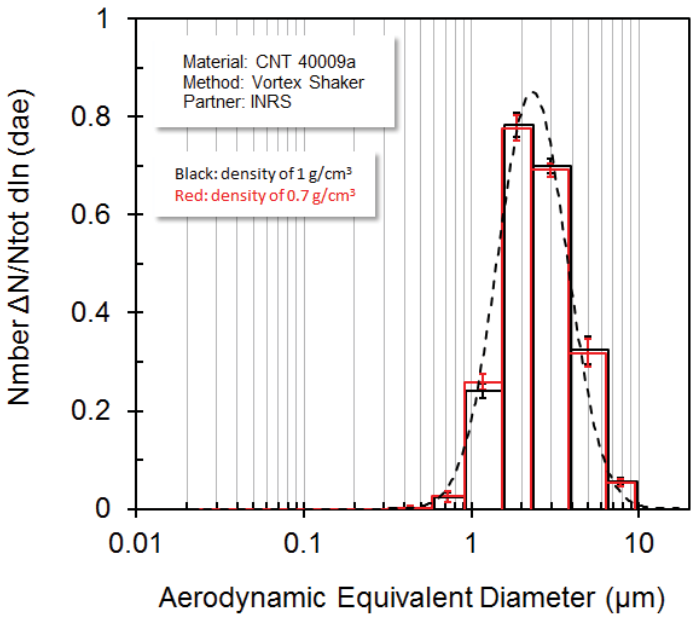

Figure 21: Number-weighted size distribution versus aerodynamic equivalent diameter time-integrated over the period of vibration (60 s) for the CNT 40009a. Histogram is presented for two densities (1 and 0.7 g/cm^3); average values are shown with their standard deviation over 3 experiments. Dotted line corresponds to the fitted distribution obtained for the density of 1 g/cm^3.

Table 4: Characteristics of fitted distributions on the number-weighted size distributions obtained with the ELPI. *ND stands for Not Determined. Mode 1 corresponds to the highest mode and mode 2 to the lowest mode of the fitted distribution.*

#	Carbon nanotube			Modes of the fitted distribution		
	Type	Code	MW or SW	Number of modes	Mode 1	Mode 2
1	Core	NM 400	MW	ND		
2		NM 401		ND		
3		NM 46000a	SW	ND		
4	Alternative	NM 402	MW	ND		
5		NM 403		ND		
6		NM 40001a		2	0.057	2.05
7		NM 40002a		2	1.86	0.13
8		NM 40003a		2	2.46	0.14
9		NM 40004a		1	1.94	-
10		NM 40005a		1	1.94	-
11		NM 40006a		1	2.23	-
12		NM 40007a		1	1.90	-
13		NM 40008a		2	1.90	0.15
14		NM 40009a		1	2.31	-

Figure 22, Figure 23, Figure 24, Figure 25 and Figure 26 present selected TEM images of airborne CNT collected with the MPS system as explained in the paragraph 2.3.1.1. The MWCNT 401 was chosen for its singular morphology, the SWCNT 46000a because it is the only one SWCNT of the series and the NM 400, NM 40001a, NM 40002a because there are well representative of the others CNTs.

The images located at the top left of each figure shows the structure of the square mesh grid (openings of 40 x 40 µm2) with collected particles. These images first suggest that the protocol used makes it possible to obtain TEM grids which are not overloaded, i.e. that the number of particles per unit of area allows straightforward observation.

The images also illustrate that the particles that compose the aerosols released varied greatly in terms of size and morphologies of the CNTs aggregate structures. In all of the images observed, only the MWCNT 401 showed individual fibers, and some of them seem to be knotted, as shown in Figure 26. The rest of the images obtained for all CNTs present nanotubes having different diameters and aspect ratios that are tied or wrapped up together in bundles. These bundles have different shapes and their sizes spread over the range from few tens of nm up to several tens of micrometers. Of these bundles more or less dense, many nanotubes are generally protruding,

which are either straight or curved. A closer examination of the bundles shows the presence of metal catalyst particles attached to some of the nanotubes, and EDS analysis indicates that it is essentially Fe.

The images shown in the below Figures give descriptive elements which remain therefore very qualitative. It was not the goal to go any further. Nevertheless, it would be interesting to link the data obtained in the Table 4 with these observations.

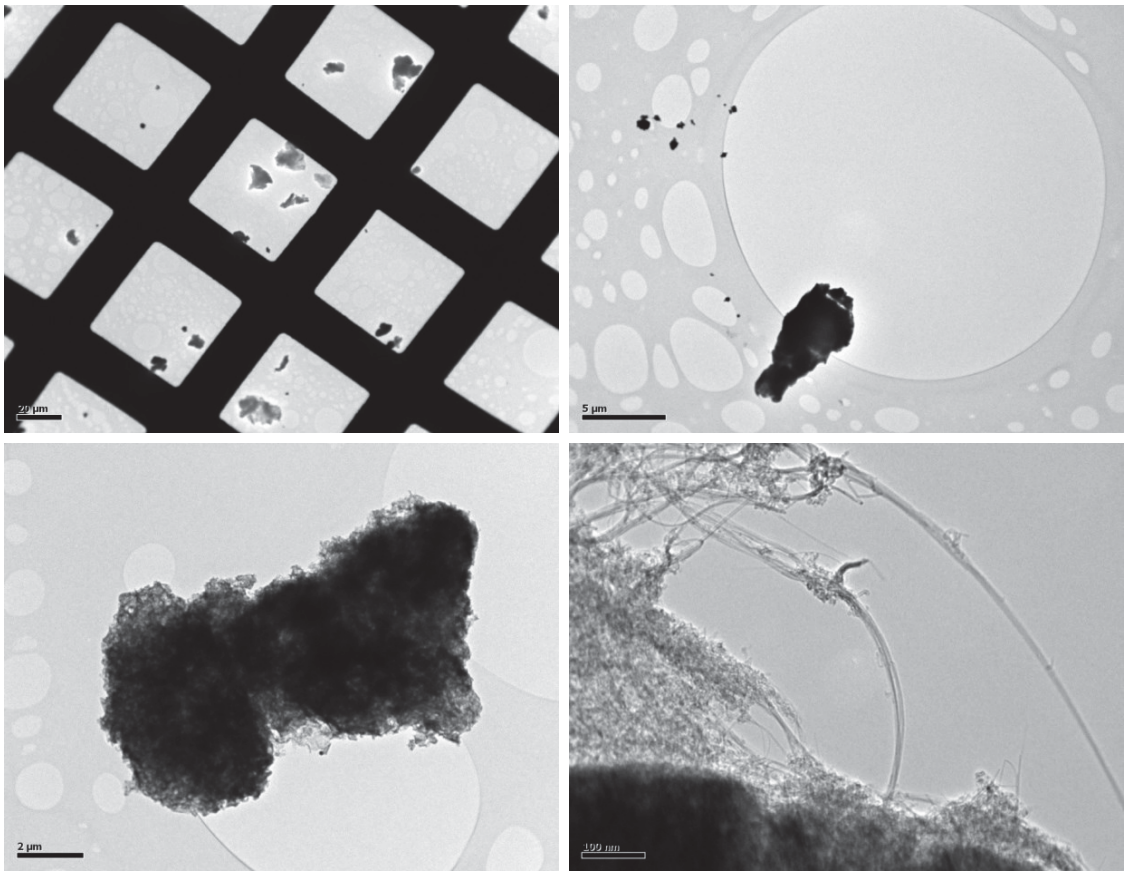

Figure 22: TEM images of airborne CNT sampled during the SWCNT 46000a Vortex Shaker experiments. Sampling duration of 10 s with the MPS equipped with 400 mesh Holey Carbon Film TEM grids. Images made by LEPI for INRS.

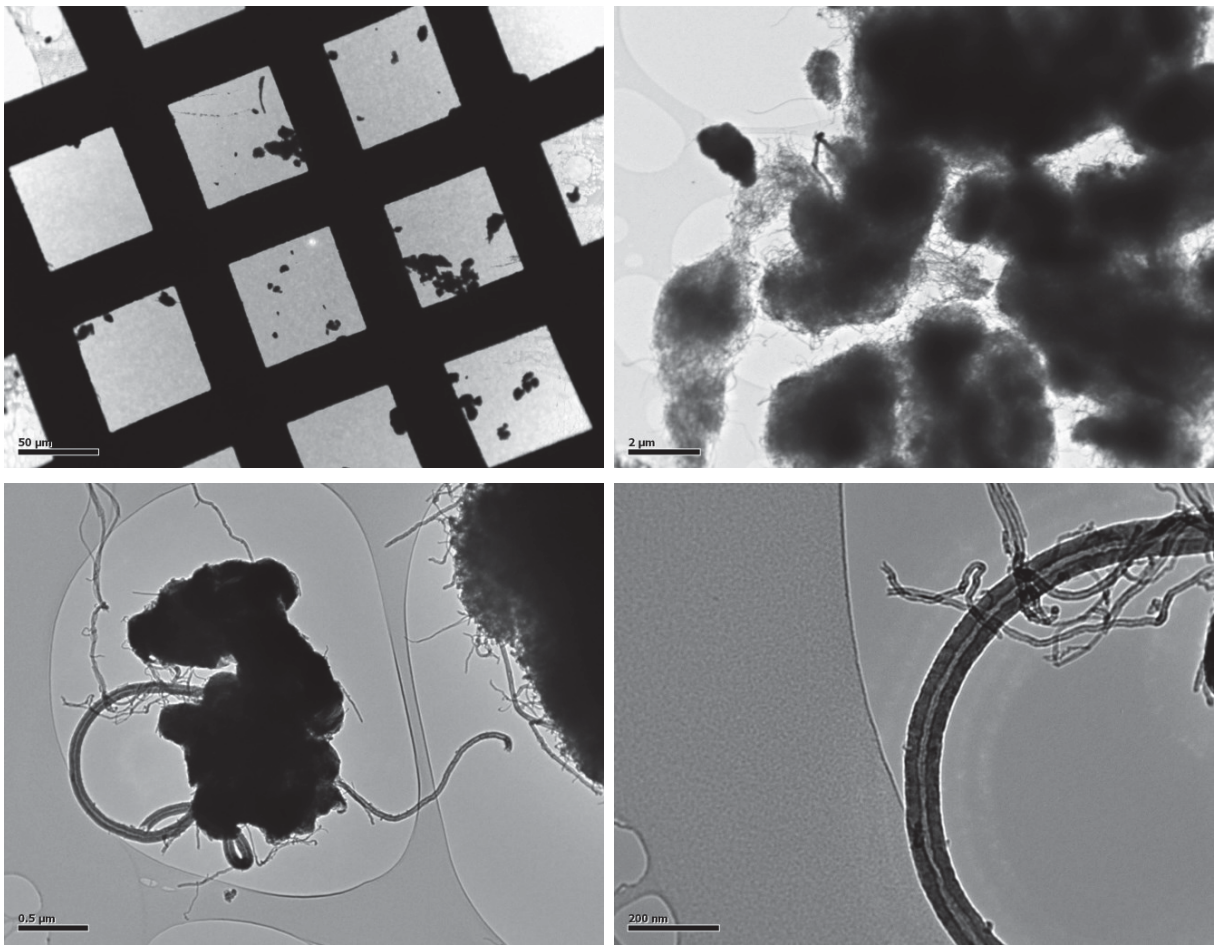

Figure 23: TEM images of airborne CNT sampled during the MWCNT 40001a Vortex Shaker experiments. Sampling duration of 10 s with the MPS equipped with 400 mesh Holey Carbon Film TEM grids. Images made by LEPI for INRS.

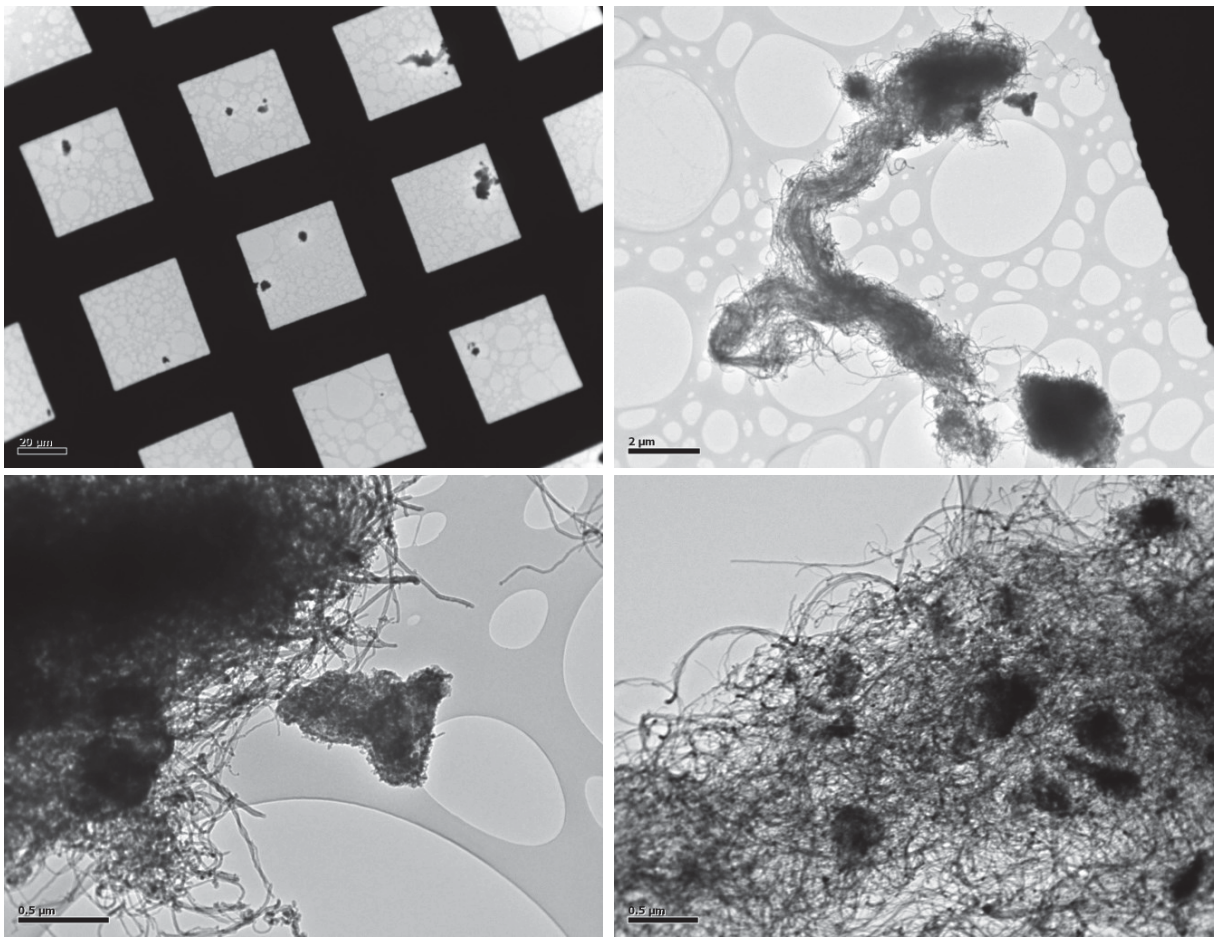

Figure 24: TEM images of airborne CNT sampled during the MWCNT 40002a Vortex Shaker experiments. Sampling duration of 10 s with the MPS equipped with 400 mesh Holey Carbon Film TEM grids. Images made by LEPI for INRS.

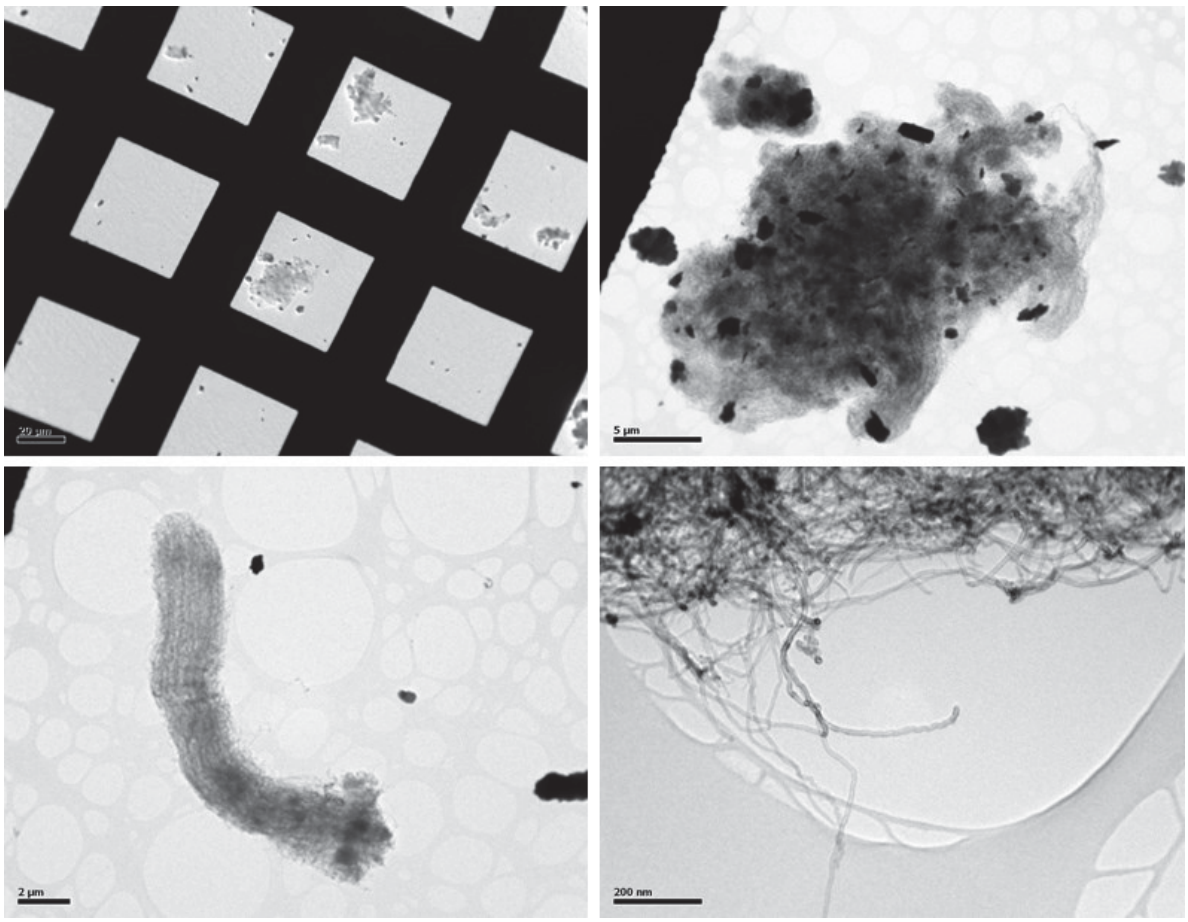

Figure 25: TEM images of airborne CNT sampled during the MWCNT 400 Vortex Shaker experiments. Sampling duration of 10 s with the MPS equipped with 400 mesh Holey Carbon Film TEM grids. Images made by LEPI for INRS.

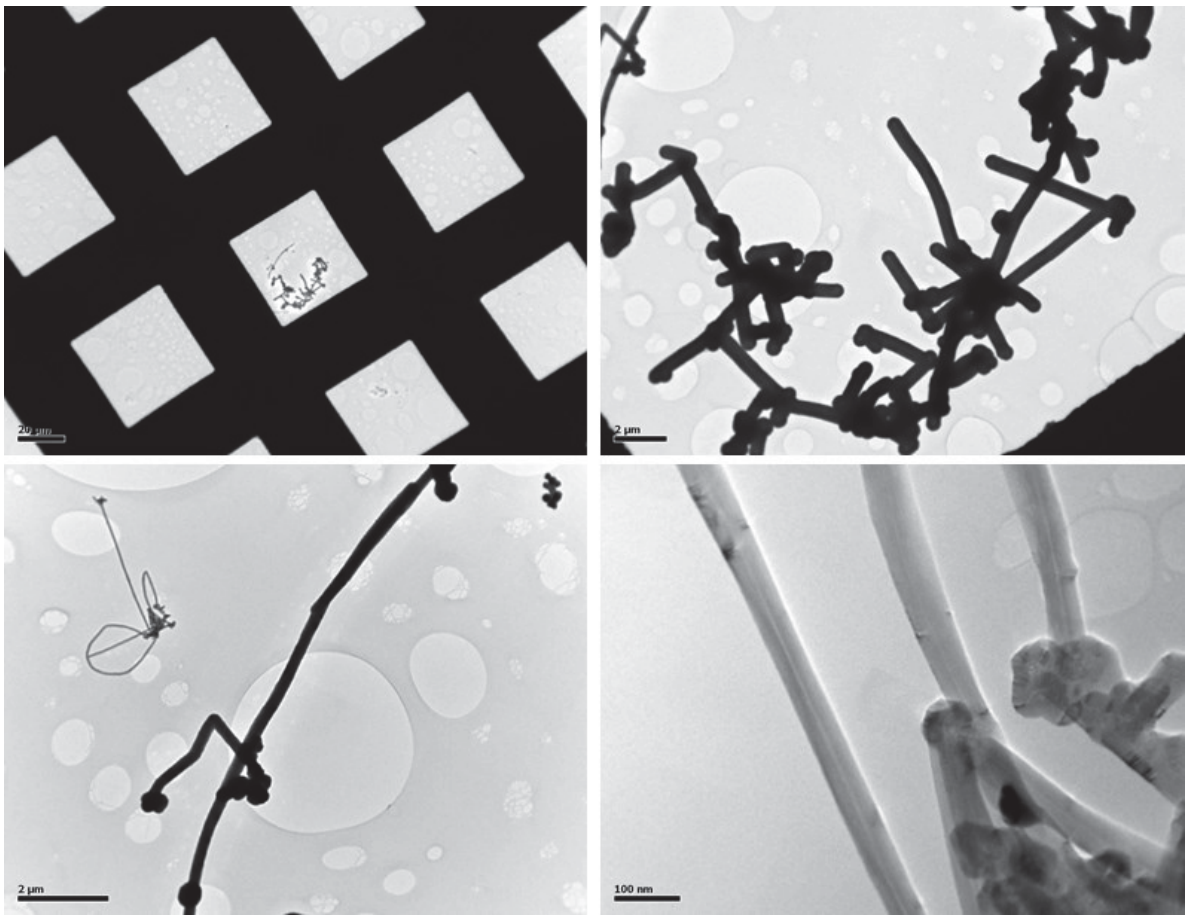

Figure 26: TEM images of airborne CNT sampled during the MWCNT 401 Vortex Shaker experiments. Sampling duration of 10 s with the MPS equipped with 400 mesh Holey Carbon Film TEM grids. Images made by LEPI for INRS.

In conclusion, the VS method, as developed in this project, gives reproducible results both in terms of amount (mass-based or number-based) and number size distributions of the generated CNT. The number-based and mass-based dustiness indices of the investigated CNTs present a large span over several orders of magnitude. It is interesting to note that ranking is different if we take as reference the number or mass parameter. Released aerosols are polydisperse with number-weighted size distributions covering the range from about 50 nm to about 10 µm in aerodynamic equivalent diameter. These results are confirmed qualitatively by electron microscopy observations.

2.4.2 *Small Rotating Drum (SRD) method*

The data presented in this paragraph are from NRCWE.

Table 5 shows the respirable dustiness indices of the three CNTs tested by the SRD at NRCWE and Table 6 shows the number of particle released during 60 seconds rotation and the subsequent 120 seconds post-rotation sampling of the dust cloud. Both the gravimetric dustiness indices and released particle numbers are relatively comparable with the respirable dustiness being slightly higher for NM 400. Considering the number dustiness index, NM 401 produces by far the highest number of particles while NM 400 the lowest.

Table 5: Mass-based dustiness index in mg/kg obtained with the SRD method for the three tested CNT.

#	Carbon nanotube			Mass-based dustiness index (mg/kg)
	Type	Code	MW or SW	
1	Core	NM 400	MW	32.0 (5.9)*
2		NM 401		23.8 (5.8)
3		NM 46000a	SW	24.2 (1.6)

*Calculated based on two values, as the third value is seven times higher. This is because all the values are under the detection limit of our gravimetric weighing system.

Table 6: Number of particles released overs 180 s obtained with the SRD method for the three tested CNT.

#	Carbon nanotube			Number of particles released over 180 s (-)
	Type	Code	MW or SW	
1	Core	NM 400	MW	6.08e+09
2		NM 401		1.79e+10
3		NM 46000a	SW	1.44e+10

Figure 27, Figure 28 and Figure 29 show plots of the evolution in the total number concentration during dustiness testing of the three CNTs. The plots show that the test gives consistent results through all three tests. The operational conditions are 50 % RH and 11 l/min flow through dustiness drum. The results, however, show that the CPC 3007 gives much lower number concentrations than the results measured with ELPI. Therefore the CPC data were not used in the data analysis. As the system is still in a draft standard configuration, it has been realized that the sampling train should be further optimized and the sampling positions for the instruments changed in order to get better agreement between the CPC 3007 and ELPI+.

The aerodynamic number size distributions measured with ELPI+ are presented in following same figures. As observed for the total number concentration data integrated from ELPI+, the number size-distribution spectra's are also quite comparable between the three CNTs. However, it is not clear whether the lover peek around 30 nm is real or due to instrumental error.

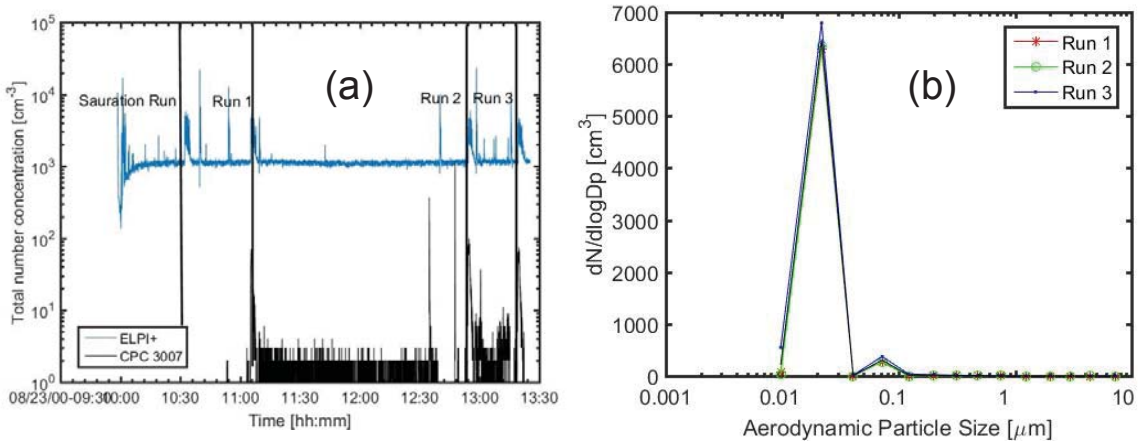

Figure 27: Time profile of the number concentration (a) and number-weighted size distribution versus aerodynamic equivalent diameter (b) obtained with the MWCNT 401.

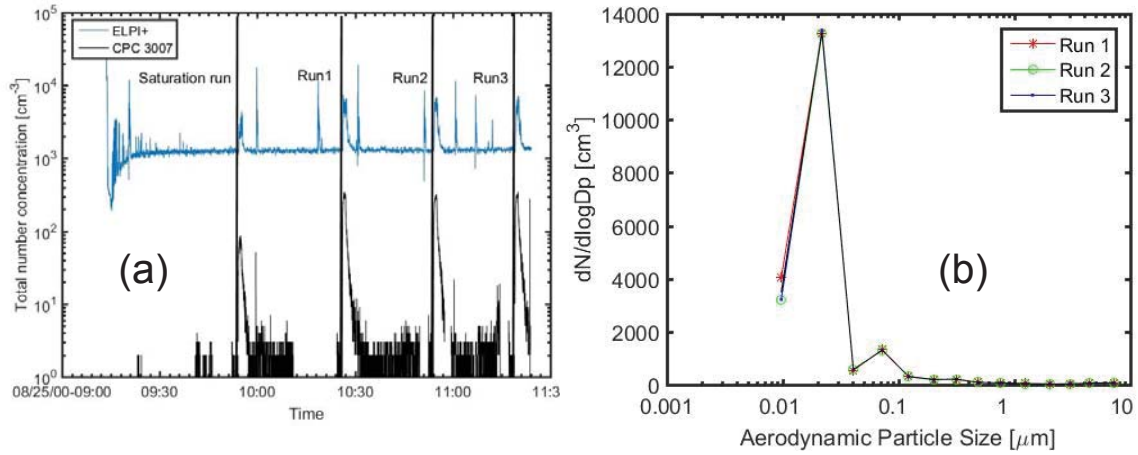

Figure 28: Time profile of the number concentration (a) and number-weighted size distribution versus aerodynamic equivalent diameter (b) obtained with the MWCNT 400.

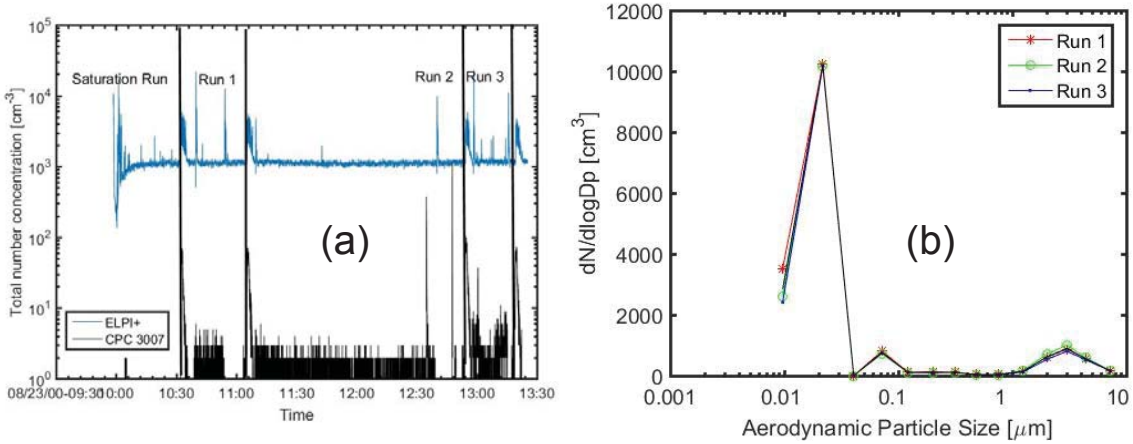

Figure 29: Time profile of the number concentration (a) and number-weighted size distribution versus aerodynamic equivalent diameter (b) obtained with the SWCNT 46000a.

During this work it became apparent that the design of the sampling line had to be revised. Therefore, these results obtained in the context of NanoREG should be taken as preliminary results.

2.4.3 *Vibrofluidization (VF) method*

Dustiness testing with NM 400

Observation of powder bed states

The state of the powder bed during dust generation could be determined by exchanging the pipe part of the container made of aluminum (ISO-KF SC52KA, see Figure 9 (b)) with a part made of glass, since a fluidized bed showed bed extension. Flow rate and frequency of the shaker were varied to assess at which operational conditions a fluidized bed would be established. The particle number concentration was observed over the course of this assessment. 450 g of NM 400 were applied to the container. Three states of the powder bed could be observed:

1. $Q_a = 0$, $f_\sim = 0$: Fixed powder bed with a bed height of 20 mm. This powder state is shown in Figure 30 (a).

2. $Q_a < 0.25\ \mathrm{L/min}$, $f_\sim < 30\ \mathrm{Hz}$: This state exhibits macroscopic spherical agglomerates of powder grains, 1-3 mm in diameter, bouncing on the powder bed and colliding with the walls and each other. This powder bed state is shown in Figure 30 (b) with $Q_a = 0.1\ \mathrm{L/min}$ and $f_\sim = 20\ \mathrm{Hz}$.

3. $Q_a > 0.25\ \mathrm{L/min}$, $f_\sim > 30\ \mathrm{Hz}$: Clear bed extension could be observed, as shown in Figure 30 (c) in which the powder bed had a height of ca. 26 mm at $Q_a = 0.3\ \mathrm{L/min}$ and $f_\sim = 40\ \mathrm{Hz}$

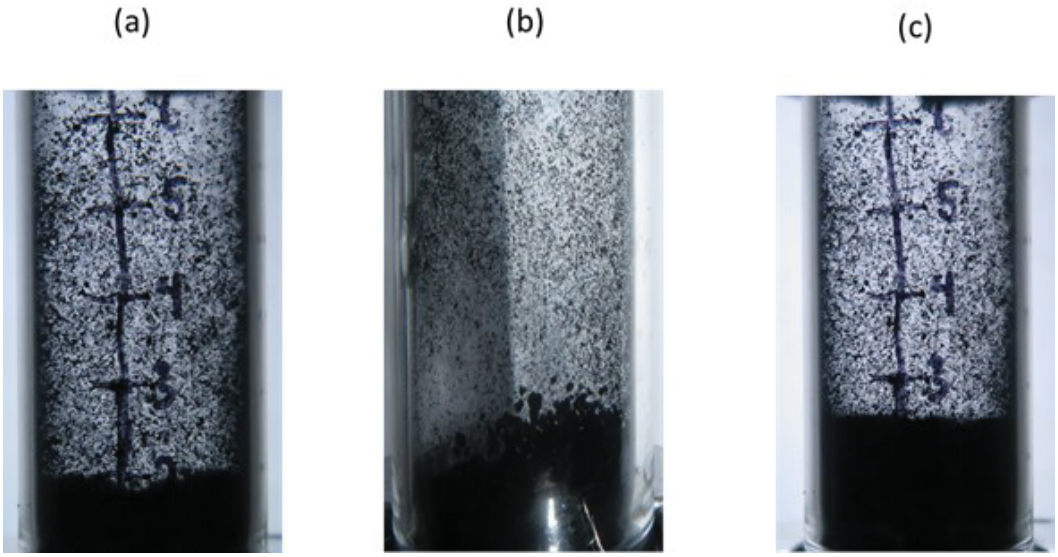

Figure 30: Different states of the powder bed during the VF-method: (a) Fixed bed, (b) Tangled bed, (c) Fluidized bed.

The powder bed states shown in Figure 30 (a) and (c) are clearly identifiable following the criteria mentioned in section 2.3.3 as the fixed bed and the (vibro)-fluidized bed and can be explained with conventional fluidization theory. However, to the author's knowledge, the state shown in Figure 30 (b) has not been observed yet.

Without additional experiments, the reason for the occurrence of this state cannot be properly explained. However, an early hypothesis assumes that due to the movement of the grains on the surface of the powder bed, smaller aggregates becomes entangled to larger "host"-aggregates like snowflakes become attached to a snowball. Constant entanglement leads to larger "ball"-like aggregates. This powder state is henceforth called tangled bed due to the lack of a better term.

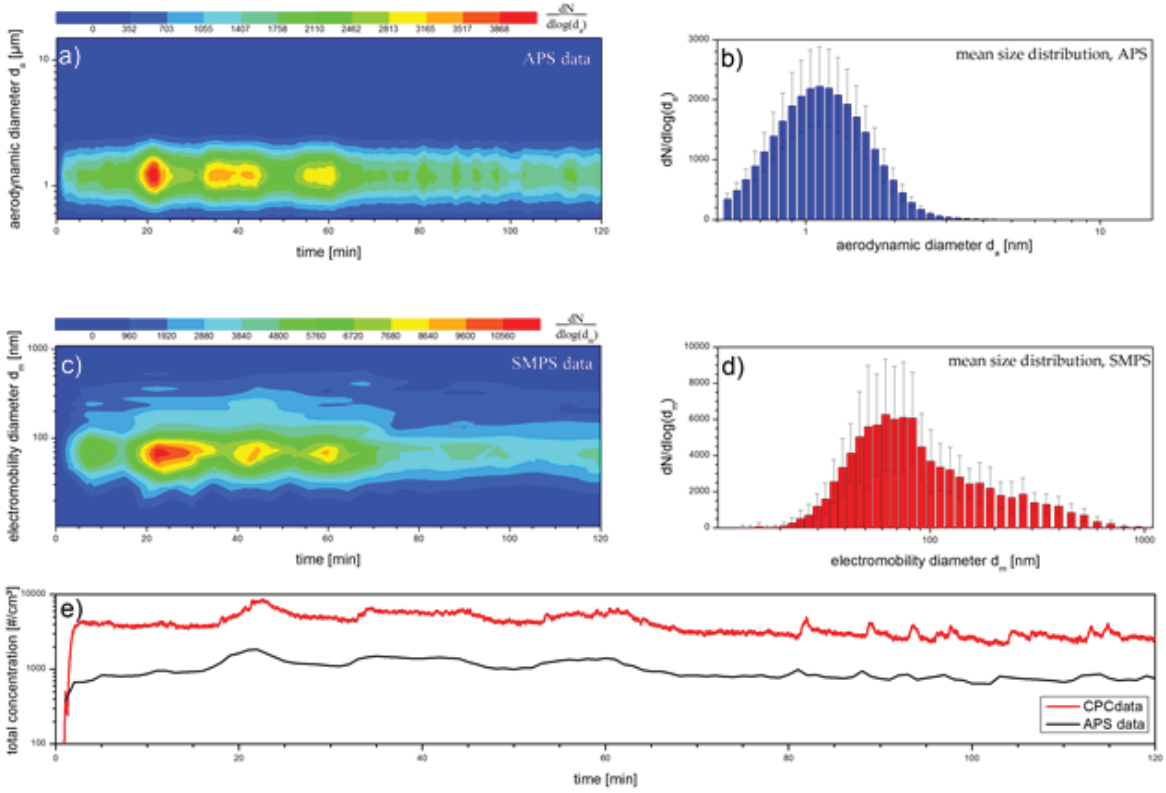

Figure 31: Dustiness profile of the tangled bed of NM 400. (a) APS particle size distribution as a function of time. (b) APS mean particle size distribution. (c) SMPS particle size distribution as a function of time. (d) SMPS mean particle size distribution. (e) CPC particle number concentration as a function of time.

Dustiness profiles for the tangled and fluidized bed

Figure 31 shows the dustiness profile of NM 400, when the powder bed was tangled. The operational conditions were $Q_a = 0.1\ \mathrm{L/min}$, $f_\sim = 20\ \mathrm{Hz}$ and $U_\sim = 4\ \mathrm{V}$. Both the APS and SMPS show log-normally distributed particle sizes (Figure 31 (b) and (d)) emitted during the dustiness test which indicates that the emitted aerosol consisted of an ultra-fine fraction and a fine fraction. The particle number concentration was not consistent over the course of the dustiness test. Both the APS and SMPS measured fluctuations of the dust emissions in terms of number, whereas the mean particle size did not change. Fitting the data with the lognormal impulse function (see section 2.3.3.3) revealed that the ultra-fine size distribution could be described with an enveloping curve made of two individual impulse curves.

To determine the morphology of the emitted particles, dust was collected on nucleopore filters and analyzed by scanning electron microscopy (SEM). Figure 33 shows images of typical morphologies found in NM 400 aerosols. Both agglomerates (Figure (a)-(c)) and single fibers (Figure 33 (d)) were found. Aggregates occurred as low-aspect-ratio particles (Figure 8 (c)) as well as high-aspect-ratio fiber aggregates (Figure 33 (a) and (b)). All aggregates were in the size range of 3-10 µm (e.g. length). From this analysis, it was determined most probable that the ultra-fine fraction measured with the CPC and SMPS consisted of single fibers whereas the APS only detected the large aggregates.

As explained in chapter 0, the number-based and mass-based dustiness index was determined using only the data from the CPC monitoring of the particle number concentrations and hence only comprised single fibers. Table 7 gives a summary on the dustiness indices and the size data of the dust emitted from the tangled bed under the operational conditions stated above.

Figure 32 shows the dustiness profile of NM 400 for the case of a (vibro)-fluidized bed. The operational conditions were $Q_a = 0.3\ \mathrm{L/min}$, $f_\sim = 40\ \mathrm{Hz}$ and $U_\sim = 4\ \mathrm{V}$. Table 1 gives a summary on the data obtained in this evaluation. Again, both the APS and SMPS showed particle size distributions that can best be fitted with lognormal impulse functions, in case of the SMPS data with an enveloping curve made of two individual impulse curves. The mean sizes of the modes are smaller compared to the case of the tangled bed, but not significantly. SEM images show particles with morphologies similar to the particles depicted in Figure 33. However, the emitted particle number concentration is one order of magnitude lower. Consequently, the dustiness indices are smaller compared to the tangled bed case. Curves of the measured particle number concentrations of the ultra-fine and fine fraction are much smoother and the magnitudes of emission stable over time, compared to the case of the tangled bed (the peaks in the APS data is due to instrument errors and were consistently occurring during the measurements).

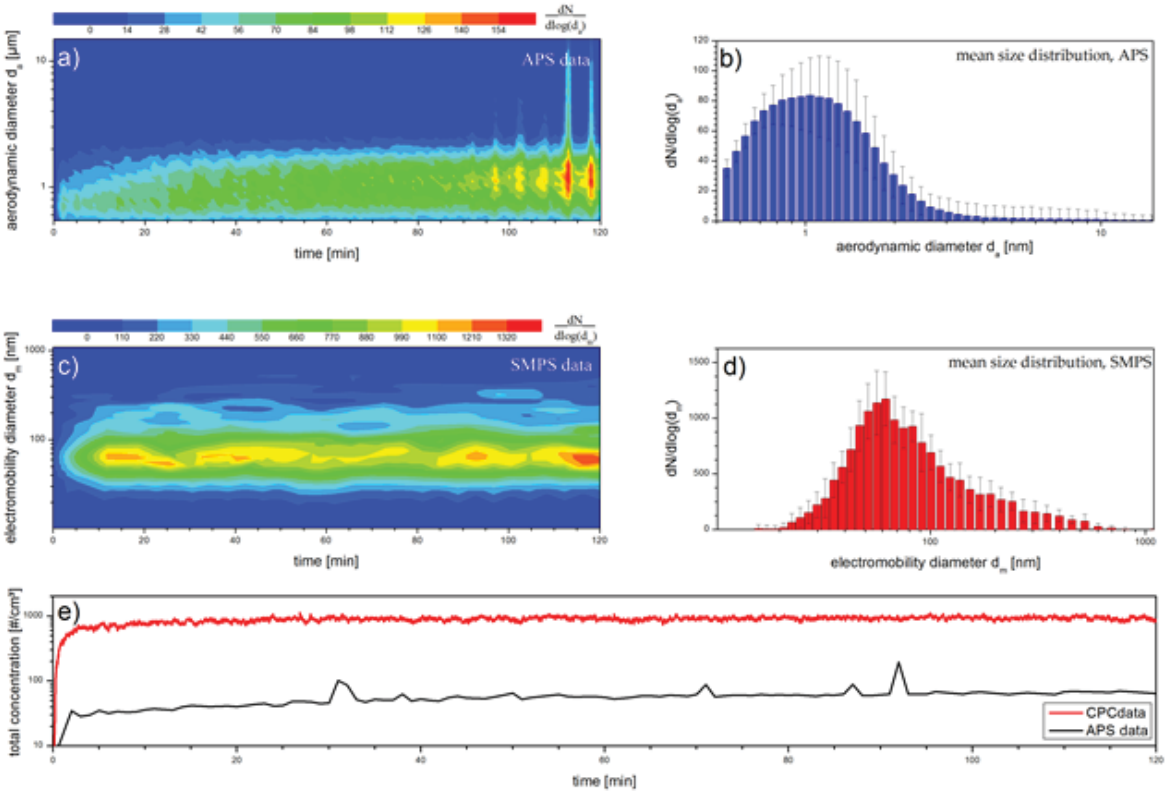

Figure 32: Dustiness profile of the (vibro)-fluidized bed of NM 400. (a) APS particle size distribution as a function of time. (b) APS mean particle size distribution. (c) SMPS particle size distribution as a function of time. (d) SMPS mean particle size distribution. (e) CPC particle number concentration as a function of time.

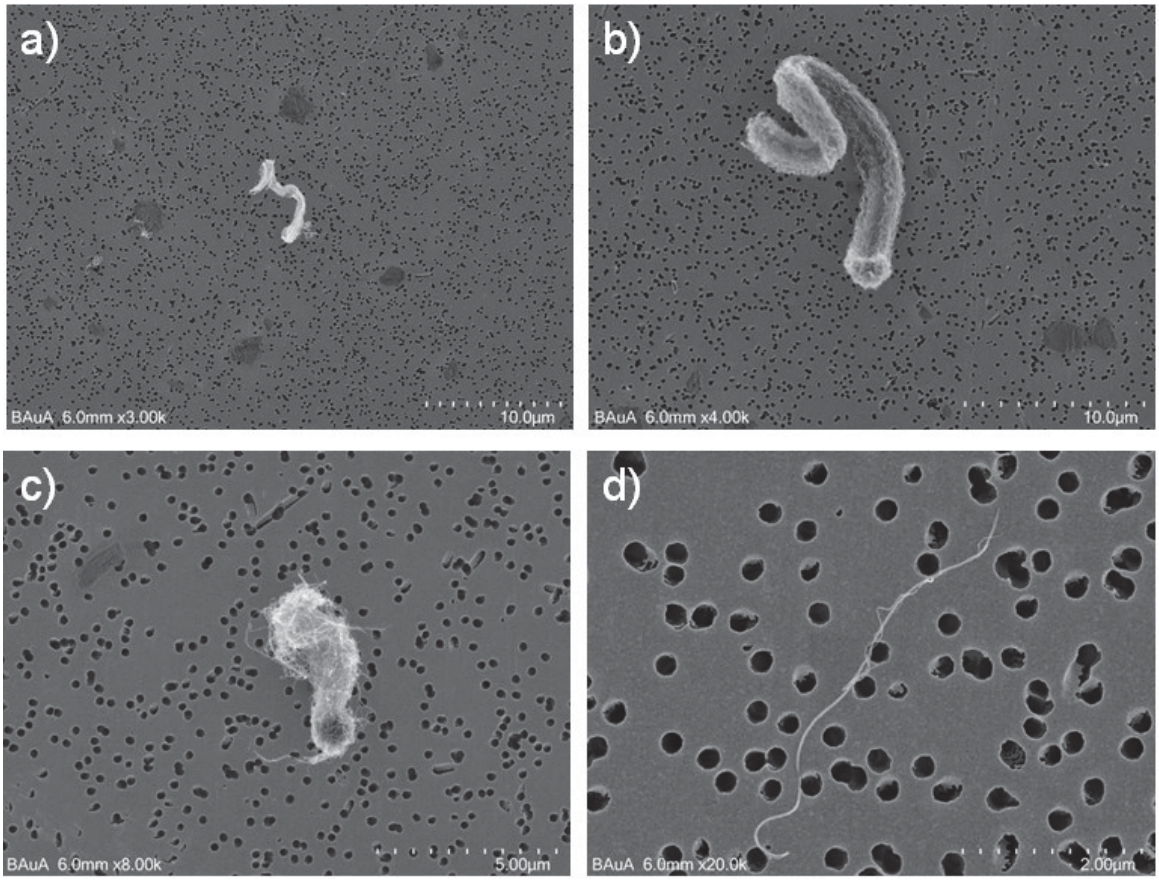

Figure 33: SEM images of NM 400 particles collected on nuclear pore filter samples (0.1 L/min, 20 Hz, 4 V).

Table 7: Dustiness indices of NM400 tested for 2 h with 0.1 L/min, 20 Hz, 4 V (tangled) and 0.3 L/min, 40 Hz, 4 V (fluidized).

	Dustiness index [1/mg]	Dustiness index [mg/kg]	Number of modes	Size of the highest mode	Size of the 2nd mode	Size of the 3rd mode
NM 400 (tangled)	3,81E+08	111,81	3	0.061 µm	0.170 µm	1.117 µm
NM 400 (fluidized)	1.5E+08	21.5	3	0.058 µm	0.127 µm	1.001 µm

Dustiness testing with NM 401

Observation of the powder bed state

Under the operating conditions available, no (vibro)-fluidized bed could be observed. Apart from the fixed bed, the tangled bed was established, with “ball”-like aggregates with diameters of 3-8 mm, hence larger than those for NM 400.

Dustiness profiles for the tangled bed

Figure 34 shows the dustiness profile for NM 401 for the case of a tangled bed, when the operating conditions were $Q_a = 0.1\ \mathrm{L/min}$, $f_\sim = 20\ \mathrm{Hz}$ and $U_\sim = 4\ \mathrm{V}$.

Table 8 gives a summary of the results of the data evaluation. An individual size distribution could be detected with the SMPS, but not a full size distribution with the APS. The particle number concentration peaked initially, but settled to a constant value.

Figure 35 shows SEM images of dust collected on nuclear pore filters during the dustiness test with NM 401. The aerosol only consisted of single fibers of small aggregates comprising a small number of fibers (Figure 35(a)-(c)). Figure 35 (d) depicts a cross-sectional view of the end of an individual fiber and shows the so-called “mega-tube” morphology of individual particles that was described in the material report of NM 401 by JRC.

From this analysis, it was concluded that both APS and SMPS detected the same aerosol fraction but at similar sizes, obviously attributable to the different size definitions (aerodynamic vs. mobility equivalent diameter). To determine the dustiness indices, only the CPC data was considered for evaluation. However, both peaks are mentioned individually in Table 8.

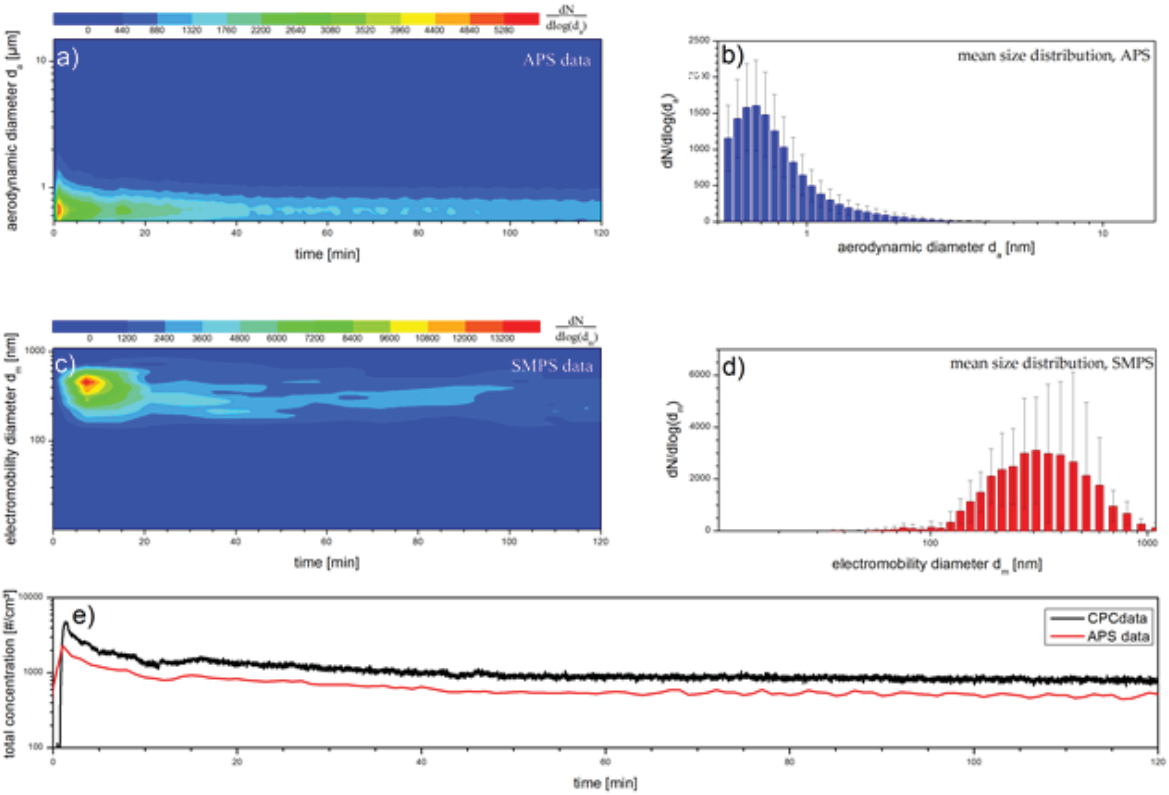

Figure 34: Dustiness profile of the tangled bed of NM 401. (a) APS particle size distribution as a function of time. (b) APS mean particle size distribution. (c) SMPS particle size distribution as a function of time. (d) SMPS mean particle size distribution. (e) CPC particle number concentration as a function of time.

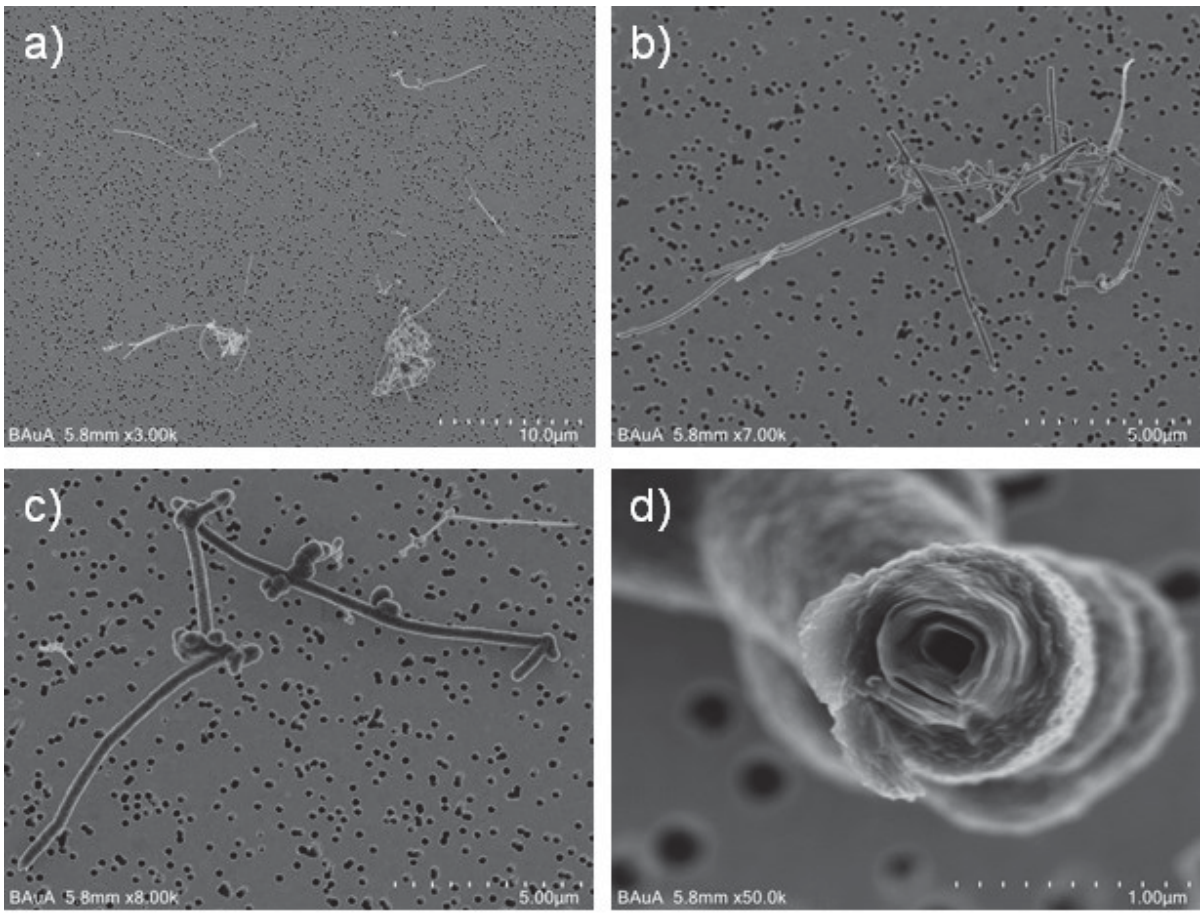

Figure 35: SEM images of NM 401 particles on nuclepore filter samples (0.1 L/min, 20 Hz, 4V).

Table 8: Dustiness indices of NM401 tested for 2 h with 0.1 L/min, 20 Hz and 4V.

	Dustiness index [1/mg]	Dustiness index [mg/kg]	Number of modes	Size of the highest mode	Size of the 2nd mode	Size of the 3rd mode
NM401	3,91E+08	9756	2	0.329 µm	0.651 µm	

Conclusion

The dustiness tests with the Vibrofluidization method revealed that two different states of the powder bed could be established, apart from the initial fixed bed.

For both NM 400 and NM 401, tangled beds could be observed, showing the entanglement of smaller aggregates on larger host aggregates. Particles are most likely emitted by collision of these macroscopic aggregates with walls and other aggregates. The dust generation was highest when the powder bed was in the tangled bed. The tangled bed seems to be only occurring for fibrous materials since it has not previously been observed for powders of conventional materials and nanomaterials.

Only occurring for higher flow rates and higher frequencies, fluidized beds were observed for NM 400, where a clear bed extension was visible. Dust generation was lower when compared to the case of the tangled bed, even if the flow rate was three times as high.

2.4.4 *Comparison between the methods*

Given that (1) the methodologies used, (2) as well as the way the data were presented were different , and (3) the small number of CNT in common (NM 400 and 401) between the methods, a comparison between the three methods could not be carried out.

What can be noted however is that electron microscopy images obtained (by TEM for INRS and SEM for BAuA) show objects similar in size and shape.

The comparison being thus extremely limited, a review of the existing data with which a possible comparison could be made was undertaken. Although a number of experimental studies have been carried out on the dustiness of carbon nanotubes [6], only two of them have produced dustiness results that can be compared to the results of this work [27, 33]. The data available for comparison are shown in Figure 36.

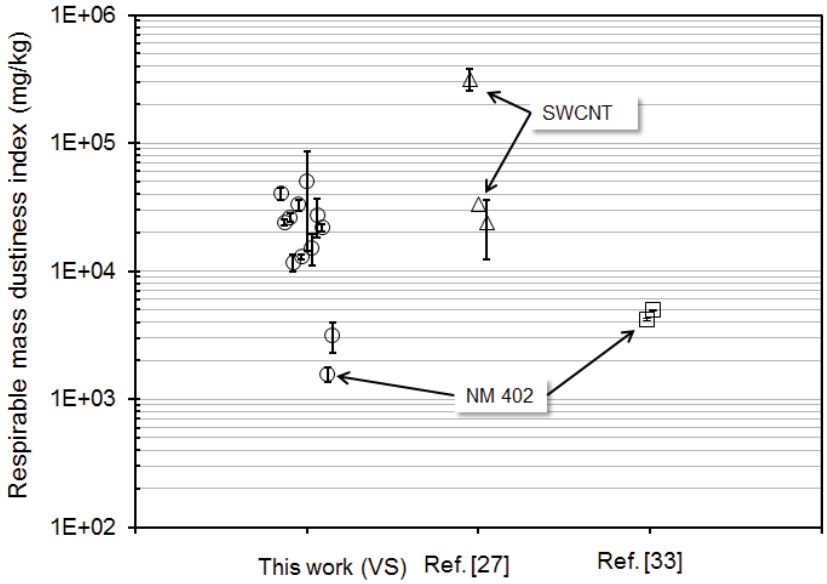

Figure 36: Comparison of the respirable mass-based dustiness indices (in mg/kg) obtained in this work and the published available indices from [27, 33].

In one of the studies, the dustiness test method used is somewhat different to the VS as the method is based on the Venturi dustiness testing device developed initially for pharmaceutical powders [26], while in the other study the dustiness method is also based on a vortex shaker but with a different configuration and measurement protocol [33]. Moreover, the trade names from the JRC CNT samples cannot be known, while the names are given for the three CNTs used in one of

the other studies [27]. That is why interpretation on the comparison can only be very limited. Among all the dustiness values obtained with the VS method (see Figure 14), only two of them are categorized as SWCNT. Overall, the dustiness values cover a little more than two orders of magnitude, between about ~1.6 10^3 mg/kg up to about ~3.2 10^5 mg/kg. Interestingly, only one link can be made on NM 402. The difference between the two $DI_{M,R}$ for NM 402 is quite important as the value obtained in this work is ~20 times lower than the value obtained in the previous study [33]. This is essentially due to a difference in the test protocol. Indeed, in the previous study, bronze micro-beads were added to the test samples in the cylindrical tube so as to favor de-agglomeration and release of airborne particles during the agitation. Moreover the test sequence was based on 3600 s of agitation and sampling, thus very different from the protocol used in this work.

2.5 Evaluation and conclusions

The objectives to this work were:

- To develop further the Vortex Shaker (VS) and Small Rotating Drum (SRD) dustiness methods, two methods that have been the focus of attention for few years in various EU projects, including an on-going standardization CEN project [24, 36].

- To develop a new method, referred to as the Vibrofluidization (VF) method.

These developments were to apply within the framework of the NanoREG project to the case of carbon nanotubes. The main reason was that handling of CNT is a plausible scenario over their entire life-cycle, but for which exposure data obtained at workplaces are unfortunately scarce. Thus, it was hoped that the dustiness data produced could feed the future risk assessments by providing input parameters to exposure modeling or control banding tools.

The core multi-walled carbon nanotubes (MWCNT) NM400 and NM 401 have been tested by the three partners. The core single-walled carbon nanotube (SWCNT) NM 46000a has been tested by INRS and NRCWE. Among the alternatives MWCNT, 10 have been tested by INRS. The main reason is that the NRCWE faced experimental difficulties with the new version of the SRD test bench. Concerning the BAuA, the method being still at an initial stage, no time could be devoted for testing other CNTs.

New parameters are proposed in this work to determine the dustiness of powders, including the number- and mass-based dustiness indices. This has been applied to all three methods.

Overall, results show quite good reproducibility for each method.

For the VS method, the dustiness indices spread over a wide range of 2 and 3 orders of magnitude for mass and number metrics, respectively, suggesting a corresponding significant difference in terms of potential (for) exposure. Also, the ranking is different whether the two dustiness metrics are considered, with no correlation between them. Electron microscopy observations show that CNTs are mostly released as bundles of different shapes and sizes that spread over the range from few tens of nanometers up to several tens of micrometers. From these bundles, several individual nanotubes are generally protruding.

At this stage, it is necessary to reiterate here that each dustiness method developed (in this project, but also in others projects) is supposed to simulate a scenario of exposure in particular. The aim is not, therefore, to have only one dustiness method but several at the disposal of users. Thus the users will be able, according to their manipulation envisaged, to choose the most appropriate dustiness method. The important thing is therefore that the dustiness is determined in these different methods according to the same procedure in terms of powder conditioning, experimental conditions, measurement strategy and expression of the results. Thus, the data can be used in a similar way, as input parameters, in to exposure modeling or control banding tools. This harmonization is also crucial for the establishment of database on dustiness.

A first step towards harmonization was taken in this project as well as in the on-going standardization CEN project [24, 36] in which two others dustiness method are included : rotating drum (RD) and continuous drop (CD) (see chapter 2.2). Thus, the experience gained in the NanoREG project with VS and SRD methods directly contributes to the ongoing development of CEN / TC 137 standards in this area. Indeed, first working drafts on the VS and SRD have been prepared by Technical Committee CEN/TC 137 “Assessment of workplace exposure to chemical and biological agents”, and the CEN enquiry should start mid-2017. Given the forthcoming publication of dedicated standards for the VS and SRD, the decision was made not to produce SOPs.

Regarding the VF method, the situation is different. Nevertheless, also the decision was made not to propose SOP because further experimental work must be conducted so as to have more experience feedback on a large number of nanomaterials, other than the few CNTs used in this project.

3 Deviations from the work plan

The delay is related to the fact that the experiments were conducted late for reasons of availability of test benches, real-time and sampling instruments and human resources. Furthermore, the time spent on data collection from the partners and the development of the report was underestimated by the pilot.

4 References

[1] Liden G. - Dustiness Testing of Materials Handled at Workplaces. Annals of Occupational Hygiene, 2006, 50, 437-439.

[2] Sanchez Jimenez A., Varet J., Poland C., Fern G. J., Hankin S. M., & Van Tongeren M. - A comparison of control banding tools for nanomaterials. Journal of Occupational and Environmental Hygiene, 2016, 13, 936-949.

[3] Liguori B., Hansen S. F., Baun A., & Jensen K. A. - Control banding tools for occupational exposure assessment of nanomaterials — Ready for use in a regulatory context? NanoImpact, 2016, 2, 1-17.

[4] Nakanishi J., Morimoto Y., OguraI., Kobayashi N., Naya M., Ema M., et al. - Risk Assessment of the Carbon Nanotube Group. Risk Analysis, 2015, 35, 1940-1956.

[5] CEN - Workplace exposure - Measurement of the dustiness of bulk materials - Part 1: Requirements and choice of test methods, EN 15051-1, November 2013.

[6] Jensen K., Levin M., Witschger O. - Methods for Testing Dustiness, in Nanomaterial Characterization – An Introduction, ed. Tantra, R. (Wiley & Sons), pp. 209-230.

[7] OECD (2012) Important issues on risk assessments of manufactured nanomaterials. ENV/JM/MONO(2012)8

[8] RIP-oN 2 (2011) Specific Advice on Fulfilling Information Requirements for Nanomaterials under REACH.

[9] Brouwer D (2012) Control Banding Approaches for Nanomaterials. Ann Occup Hyg, 56, 506–514

[10] Schneider T, Jensen KA (2009) Relevance of aerosol dynamics and dustiness for personal exposure to manufactured nanoparticles. J Nanopart Res, 11, 1637–1650

[11] Burdett G, Bard D, Kelly A, Thorpe A (2012) The effect of surface coatings on the dustiness of a calcium carbonate nanopowder. J Nanopart Res, 15, 1-17.

[12] Pensis I, Mareels J, Dahmann D, Mark D (2010) Comparative Evaluation of the Dustiness of Industrial Minerals According to European Standard EN 1505. Ann Occup Hyg, 54,204-216.

[13] Witschger O (2011) Monitoring Nanoaerosols and Occupational Exposure. In: Houdy P, Lahmani M, Marano F, editors. Nanoethics and Nanotoxicology. Springer Berlin Heidelberg; p. 163-99.

[14] EN 15051-2 (2013) Workplace exposure – Measurement of the dustiness of bulk materials – Part 2: Rotating drum method

[15] EN 15051-2 (2013) Workplace exposure – Measurement of the dustiness of bulk materials – Part 3: Continuous drop method

[16] Tsai, C.-J., et al. (2009) Dustiness test of nanopowders using a standard rotating drum with a modified sampling train. Journal of Nanoparticle Research, 11, 121-131.

[17] Burdett, G., et al. (2015) The effect of surface coatings on the dustiness of a calcium carbonate nanopowder. Journal of Nanoparticle Research, 15, p. 1-17.

[18] Dahmann, D. and C. Monz (2011) Determination of dustiness of nanostructured nanomaterials. Gefahrstoffe Reinhaltung der Luft, 71, 481 - 487.

[19] Baron PA, Maynard AD, Foley M. (2002) Evaluation of aerosol release during the handling of unrefined single walled carbon nanotube material. Cincinatti, Ohio, USA: National Institute of Occupatonal Safety anf Health; Report No.: DART-02-191.

[20] Ogura I, Sakurai H, Gamo M. (2009) Dustiness testing of engineered nanomaterials. Journal of Physics: Conference Series 2009;170(012003):1-4.

[21] Witschger O, Bianchi B, Bau S, Levin M, Koponen IK, Jensen KA. (2012) Key intrinsic physicochemical characteristics of NANOGENOTOX nanomaterials - Deliverable 4.6: Dustiness of NANOGENOTOX nanomaterials using the NRCWE small rotating drum and the INRS Vortex shaker. Paris, France: French Agency for Food, Environmental and Occupational Health & Safety.

[22] Ku BK, Deye G, Turkevich LA. (2013) Characterization of a Vortex Shaking Method for Aerosolizing Fibers. Aerosol Science and Technology; 47,1293-301.

[23] Le Bihan OLC, Ustache A, Bernard D, Aguerre-Chariol O, Morgeneyer M. (2014) Experimental study of the aerosolization from a carbon nanotube bulk by a vortex shaker. Journal of Nanomaterials 2014(193154):1-11.

[24] Witschger O, Jensen KA, Brouwer DH, Tuinman I, Jankowska E, Dahmann D (2014) DUSTINANO: a CEN pre-normative research project to harmonize dustiness methods for manufactured nanomaterial powders. Aerosol Technology 2014, Karlsruhe, Abstract T230A09

[25] Plitzko, S., Gierke, E., Dziurowitz, N., Brossell, D. (2010). Generation of CNT/CNF dusts by a shaker aerosol generator in combination with a thermal precipitator as the collection system for characterization of the fibre morphology. Gefahrst Reinhalt L 70:31-35.

[26] Boundy, M., Leith, D., & Polton, T. (2006). Method to Evaluate the Dustiness of Pharmaceutical Powders. Annals of Occupational Hygiene, 50, 453-458.

[27] Evans, D. E., Turkevich, L. A., Roettgers, C. T., Deye, G. J., & Baron, P. A. (2013). Dustiness of Fine and Nanoscale Powders. Annals of Occupational Hygiene, 57, 261-277.

[28] Ding, Y., Riediker, M. (2015). A system to assess the stability of airborne nanoparticle agglomerates under aerodynamic shear. Journal of Aerosol Science, 88, 98-108.

[29] Stahlmecke,B.,Wagener,S.,Asbach,C.,Kaminski,H.,Fissan,H.,&Kuhlbusch,T.A.J.(2009).Investigation of airborne nanopowder agglomerate stability in an orifice under various differential pressure conditions. Journal of Nanoparticle Research, 1625–1635.

[30] Ding, Y., Stahlmecke, B., Jiménez, A. S., Tuinman, I. L., Kaminski, H., Kuhlbusch, T. A. J., . . . Riediker, M. (2015). Dustiness and Deagglomeration Testing: Interlaboratory Comparison of Systems for Nanoparticle Powders. Aerosol Science and Technology, 49, 1222-1231.

[31] Rasmussen K, Mech.A., Mast J, De Temmermann P-J, Waeggeners NVSF, Pizzolon JC, et al. Synthetic amorphous silicon dioxide (NM-200, NM-201, NM202, NM-203, NM-204): Characterisation and physico-chemical Properties. Luxembourg: European Union; 2013. Report No.: EUR 26046 EN.

[32] Rasmussen K, Mast J, De Temmermann P-J, Verleysen E, Waegeneers N, Van Steen F, et al. Titanium Dioxide, NM-100, NM-101, NM-102, NM-103, NM-104, NM-105: Characterisation and Physico-Chemical Properties. Luxembourg: European Union; 2013. Report No.: EUR 26046 EN.

[33] Rasmussen K, Mast J, De Temmermann P-J, Verleysen E, Waegeneers N, Van Steen F, et al. Multi-walled Carbon Nanotubes, NM-400, NM-401, NM-402, NM-403: Characterisation and Physico-Chemical Properties. Luxembourg: European Union; 2014. Report No.: EUR 26796 EN.

[34] NanoCare (2009) NanoCare Health related Aspects of Nanomaterials - Final Scientific Report. Editors: T.A.J. Kuhlbusch, H.F. Krug, K. Nau. 158 pages.

[35] ISO/TS 12025 (2012) Nanomaterials — Quantification of nano-object release from powders by generation of aerosols. 32 pages.

[36] M/461 EN (2010) Mandate addressed to CEN, CENELEC and ETSI for standardization activities regarding nanotechnologies and nanomaterials. Brussels, 2nd February 2010. 7 pages.

[37] Witschger, O., Jensen, K.A., Brouwer, D., Tuinman, I., Jankowska, E., Dahmann, D., Burdett, G., Bard D. (2014) DUSTINANO: a CEN pre-normative research project to harmonize dustiness methods for manufactured nanomaterial powders. Aerosol Technology 2014, Karlsruhe, Abstract T230A09

[38] Nowack, B., R. M. David, H. Fissan, H. Morris, J. A. Shatkin, M. Stintz, R. Zepp, and D. Brouwer. 2013. Potential release scenarios for carbon nanotubes used in composites. Environment International 59 (0):1-11.

[39] Totaro S., Cotogno G., Rasmussen K., Pianella F., Roncaglia M., Olsson H., et al. - The JRC Nanomaterials Repository: A unique facility providing representative test materials for nanoEHS research. Regulatory Toxicology and Pharmacology, 2016, 81, 334-340.

[40] Levin, M., Rojas, E., Vanhala, E., Vippola, M., Liguori, B., Kling, K., Koponen, I., Mølhave, K., Tuomi, T., Gregurec,D., Moya, S., Jensen, K. (2015). Influence of relative humidity and physical load during storage on dustiness of inorganic nanomaterials: implications for testing and risk assessment. Journal of Nanoparticle Research, 17, 337-350.

[41] Charvet, A., Bau S., Bemer D., Thomas D. (2015) On the Importance of Density in ELPI Data Post-Treatment. Aerosol Science and Technology, 49: 1263-1270.

[42] Wang, J., Y. K. Bahk, S.-C. Chen, and D. Y. H. Pui. 2015. Characteristics of airborne fractal-like agglomerates of carbon nanotubes. Carbon 93:441-450.

[43] Chen, B. T., D. Schwegler-Berry, W. McKinney, S. Stone, J. L. Cumpston, S. Friend, D. W. Porter, V. Castranova, and D. G. Frazer. 2012. Multi-walled carbon nanotubes: sampling criteria and aerosol characterization. Inhalation Toxicology 24 (12):798-820.

[44] Kim, S. H., G. W. Mulholland, and M. R. Zachariah. 2009. Density measurement of size selected multiwalled carbon nanotubes by mobility-mass characterization. Carbon 47 (5):1297-1302.